DETERMINATION OF STRAIN ACCUMULATION ALONG TUZLA FAULT

by

Emre Havazlı

B.S., Geodesy and Photogrammetry Engineering, Yıldız Technical University, 2009

Submitted to Kandilli Observatory and Earthquake Research Institute,

Geodesy Department in partial fulfillment of the requirements for the degree of

Master of Science

Graduate Program in Geodesy

Boğaziçi University

2012

DETERMINATION OF STRAIN ACCUMULATION ALONG TUZLA FAULT

APPROVED BY:

Prof. Dr. Haluk Özener . . . .

(Thesis Supervisor)

Assist. Prof. Dr. Aslı Doğru . . . .

Assoc. Prof. Dr. Uğur Doğan . . . .

DATE OF APPROVAL

ACKNOWLEDGEMENTS

ABSTRACT

DETERMINATION OF STRAIN ACCUMULATION ALONG TUZLA FAULT (IZMIR)

Aegean Region is one of the most deforming parts of Alpine-Himalayan belt which is bounded by the Hellenic trench, mainland Greece and western Turkey. Anatolian plate is placed between the Eurasian and African plates. The Anatolian plate moves counter-clockwise and it is observed that the velocity of this movement grows through west. Aegean Region is an important place for geoscientists as it is a seismically active region which includes normal and lateral faults. In addition, the third biggest city in Turkey, İzmir is also settled in the region with nearly 4 million population.

This study is carried out on the Tuzla Fault which is a right lateral strike slip fault, begins from Gaziemir district and dives under the sea from the Doganbey Cape. Historical evidence shows that catastrophic earthquakes occurred on the Tuzla Fault. The Tuzla Fault has created moderate earthquakes in the past two decades and still has the potential to create large earthquakes.

The main objective of this study is to determine strain accumulation along the fault by using the results of the GPS campaigns carried out in the study area. Analysis of GPS data show that velocities reach up to 28.54 mm/yr ∓ 1.90 mm/yr. and are consistent with the present-day tectonic deformation of the region. Principal components of crustal strain along the Tuzla Fault reach up to 140 nanostrain/yr. The strain rates are in accord with seismicity and the directions of the calculated strain rates reflect the expected behavior of NE - SW extension of the Aegean Region.

ÖZET

TUZLA FAYI (İZMİR) BOYUNCA GERİNİM BİRİKİMİNİN BELİRLENMESİ

Ege Bölgesi, Helenik Yay, Yunan Anakarası ve Türkiye'nin batısı ile sınırlanmış olan ve Alp-Himalaya kuşağının en fazla deformasyona uğrayan bölümlerinden biridir. Anadolu levhası, Avrasya ve Afrika levhalarının arasında yer almaktadır. Avrasya levhası referans alındığında, Anadolu levhasının saat yönünün tersi yönünde bir hareket eğilimi içinde olduğu ve bu hareketin batıya doğru gidildikçe hızlanan bir yapıda olduğu, yapılan geniş çaplı çalışmalar ile gözlemlenmiştir. Ege Bölgesi'nin sismik olarak oldukça aktif olması ve bölgede bulunan normal ve yanal atımlı faylar nedeniyle bölge yer bilimciler için oldukça önemlidir. Ayrıca Türkiye'nin üçüncü en büyük şehri olan, yaklaşık 4 milyon nüfuslu İzmir ili, bölgede yapılan çalışmaların önemini arttırmaktadır.

Bu çalışma, Gaziemir'den başlayarak Doğanbey burnundan itibaren deniz altından devam eden, sağ yanal atımlı Tuzla Fayı üzerinde gerçekleştirilmiştir. Tuzla Fayı tarihte yıkıcı depremler üretmiştir. Yakın geçmişte orta büyüklükte depremler üreten Tuzla Fayı halen aktif ve yıkıcı deprem üretme potansiyeline sahip bir faydır.

Çalışmanın amacı; bölgede kurulmuş olan mikrojeodezik ağda yapılan GPS ölçme çalışmalarından elde edilen verilerin değerlendirilerek fay üzerideki gerinim birikiminin hesaplanmasıdır. GPS ile elde edilen verilerin analizi sonucunda, bölgede hızların 28.54 mm/yıl ∓1.90 mm/yıl değerlerine ulaştığı görülmektedir. Bu sonuçlar bölgenin günümüzdeki tektonik yapısı ile uyumludur. Hesaplanan asal gerinim elemanlarının 140 nanostrain/yıl civarında olduğu görülmüştür. Gerinim değerlerinin bölgenin sismisitesi ile uyumlu olduğu ve bölgenin tipik yapısı olan KD - GB açılmasını yansıttığı görülmektedir.

TABLE OF CONTENTS

LIST OF FIGURES

LIST OF TABLES

LIST OF SYMBOLS / ABBREVIATIONS

USGS   United States Geological Survey

GPS   Global Positioning System

CAUC   Caucasus Block

AN   Anatolian Plate

AE   Aegean Plate

Ma   Million Years

M   Magnitude

KOERI   Kandilli Observatory and Earthquake Research Institute

NEMC   National Earthquake Monitoring Center

GDMRE   General Directorate of Mineral Research and Exploration

IESEMP   İzmir Earthquake Scenario Earthquake Master Plan

GIS   Geographic Information Service

RTK   Real Time Kinematic

ASKE   Askeriye

CTAL   Çatalca

ESEN   Esenli

GEMR   Gaziemir

GORC   Görece

HZUR   Huzur Sitesi

KOKR   Kokar

KPLC   Kaplıca

PTKV   Petek Vadisi

SFRH   Seferihisar

TRAZ   Tırazlı

TURG   Turgutlu

URKM   Ürkmez

YACI	Yağcılar
YKOY	Yeniköy
AIUB	Astronomy Institute of University of Bern
MIT	Massachusetts Institute of Technology
JPL	Jet Propulsion Laboratory
NOAA	National Oceanic and Atmospheric Administration
VLBI	Very Long Base Interferometry
SLR	Satellite Laser Ranging
ITRF	International Terrestrial Reference Frame
IGS	International GNSS Service
SOPAC	Scripps Orbit and Permanent Array
E	Strain Tensor
R	Rotation Tensor
Δ	Dilatation
γ_1	Pure Shear
γ_2	Engineering Shear
γ	Shear Strain
ε_1	Maximum Principal Strain
ε_2	Minimum Principal Strain
φ	Azimuth
ψ	Shear Strain Direction
μstr	Nanostrain
FEM	Finite Element Method
TUBITAK	The Scientific and Technological Research Council of Turkey
CAYDAG	Research Group of Environment, Atmosphere, Earth and Marine Sciences

1. INTRODUCTION

The Earth's lithosphere is divided into a number of large, rigid plates (Figure 1.1) that move over a layer of the mantle known as the "asthenosphere" and interact at their boundaries. The Eurasia, the African and the Arabian plates are some of the major plates that interacts each other. They converge, diverge, or slide past one another. Such interactions are believed to be responsible for most of the seismic and volcanic activity of the Earth. According to the classical model of plate tectonics, lithospheric plates creep over a relatively plastic layer of partly molten rock known as the "asthenosphere". The lithosphere comprises the Earth's crust and the uppermost mantle, averages about 70 km thick beneath oceans and is at least 125 km thick beneath continents, while the asthenosphere extends to a depth of perhaps 200 km (Monroe, 1996).
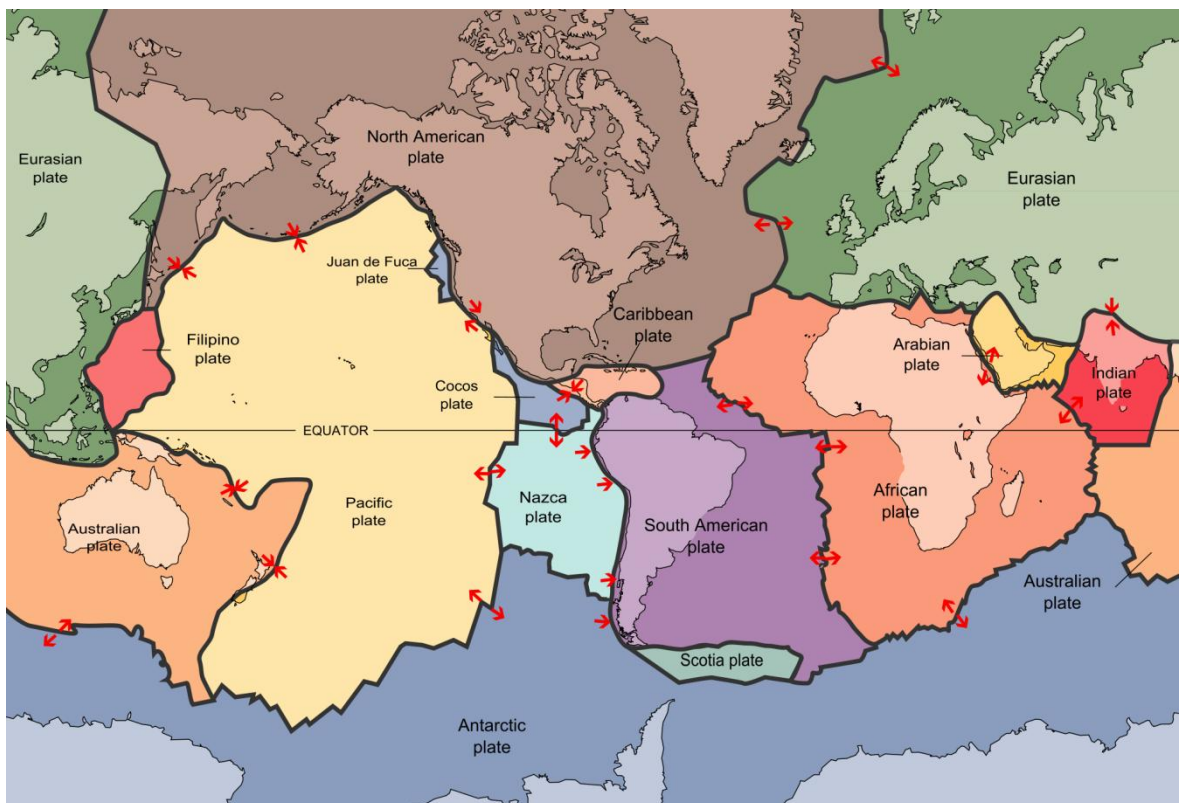
Figure 1.1. Major plates of the Earth (USGS)

The Aegean Region is one of the most seismically active regions in the world which is bounded by the African, the Eurasian and the Anatolian Plates. Several factors contribute to the deformation of the eastern Mediterranean. To the north is the stable continental interior of the Eurasia and to the south is the stable Africa (Nubia). These two tectonic plates converge at a rate of approximately 5-10 mm/yr in the eastern Mediterranean Region (Altamimi *et al*., 2002, 2007). An influx of continental lithosphere occurs from Anatolia, to the east of the Aegean. It is generally accepted that the westward motion of Anatolia and the general north-south extension that is prevalent throughout the Aegean and westernmost Anatolia is a consequence of the tectonic driving force associated with the low gravitational potential energy of the deep Hellenic subduction interface. Some authors attribute this pull to so called "trench roll back", where the motion of the subducting plate towards the subduction zone is greater than the plate convergence rate, causing the overriding crust to extend (Floyd, 2008).

Reilinger *et al.* (2006) conclude that, due to the small component of extension seen across the East Anatolian Fault, the relatively lower gravitational potential energy associated with the Hellenic bathymetric trough must be the main driving force for tectonic blocks in the wider region of the Nubia-Eurasian and Arabia-Eurasian convergence zone. This extension across the East Anatolian Fault means that it cannot be the indentation of Arabia northwards into Eurasia that is causing continental material to be extruded eastwards. This would produce compressional forces normal to the fault which would produce contraction (Floyd, 2008).

Geodetic techniques for monitoring the displacements and the deformation parameters are recognized as a favorable method in many studies focused on crustal movements. With the help of increasing knowledge on crustal deformation, the issue on understanding the behavior of interior Earth as well as the surface of it. Due to the improvements on modern technology, each survey condition had differences from the others. Therefore the triangulation and trilateration applications evolved into GPS campaigns in time.

Main concern of this thesis is determining the strain accumulation along the Tuzla Fault which is a significant fault with potential to create a large earthquake.

Geodesy Department of Kandilli Observatory and Earthquake Research Institute at Boğaziçi University is studying the Tuzla Fault since 2009. First, reconnaissance was performed in the study area in 2009 (Halicioglu and Ozener, 2008). 16 sites were established in the study area for geodynamic purposes. GPS and precise leveling surveying methods were carried out in the study area. 3 sites are chosen for precise leveling and 15 sites were used in the GPS surveys (Sabuncu and Ozener, 2010).

This study has five chapters. The second chapter of this study is about the seismicity and tectonics of the region. Besides, significant faults in the region and their locations are explained and denoted with maps in the study area. The Tuzla Fault and its features are introduced in details. Additionally, historical and instrumental period of earthquake records are placed in this chapter.

The third chapter of the study explains the basics of GPS and details of surveying campaigns. The data analyzing strategies and the GAMIT/GLOBK software is explained.

The fourth chapter gives the fundamentals of stress and strain and also their relationship. Calculation methods and results are also given in this chapter.

2. TECTONIC SETTINGS OF TURKEY AND WESTERN ANATOLIA

Over the last 200 Ma the Alpine-Himalaya belt represents the most spectacular result of the relative motion between the African and Eurasian plates. The boundary between African and Eurasian plates is delineated by the Hellenic arc and the Pliny-Strabo trench in the west and the Cyprus arc and a diffuse fault system of the Eastern Anatolian Fault Zone in the east (Yilmaz, 2000; Ergun and Oral, 2000; Kocyigit, 2000; Utku, 2000; Taymaz, 2001).

The Aegean Region forms parts of a major seismic belt - that starts at the Indian Ocean and extends up to the Atlantic Ocean - and is bounded by the African, the Eurasian and the Anatolian plates. Due to the collision of these three plates at the Aegean Region, the majority of the seismic activity of the eastern Mediterranean area occurs in the Greek territory (Jackson and McKenzie, 1988).

The Aegean Region and its surrounding area including western part of Turkey, the Aegean Sea, mainland Greece and part of the northern eastern Mediterranean is extremely seismic and active part of the Alpine-Himalayan Orogenic belt system (Mc Kenzie, 1972; Mc Kenzie, 1978; Mercier *et al*., 1977; Jackson *et al*., 1982; Armijo *et al*., 1996).

The Anatolian plate has a relative counter-clockwise motion of 22-25 mm/yr with respect to Eurasian plate. Northern part of the Africa near the Hellenic trench moves about 10 mm/yr towards north meanwhile northern Arabia plate moves with 18-25 mm/yr velocity rate with respect to Eurasia (Mc Clusky *et al*.,2000).

In addition, the Aegean Region is placed in the convergent boundary between two important plates which are African and Eurasian. During the last 92 Ma, the African plate

has activity and rotated counter clockwise with respect to Eurasian plate (Muller *et al*.,1993). Thus the Aegean Region is dominated by pure shear stress and the deformation is relative to the Eurasia with counter-clockwise rotating Anatolian plate. Aegean Region with 30 mm/yr NE-SW extension is very active continental extension in the world (Mc Clusky *et al*.,2000).
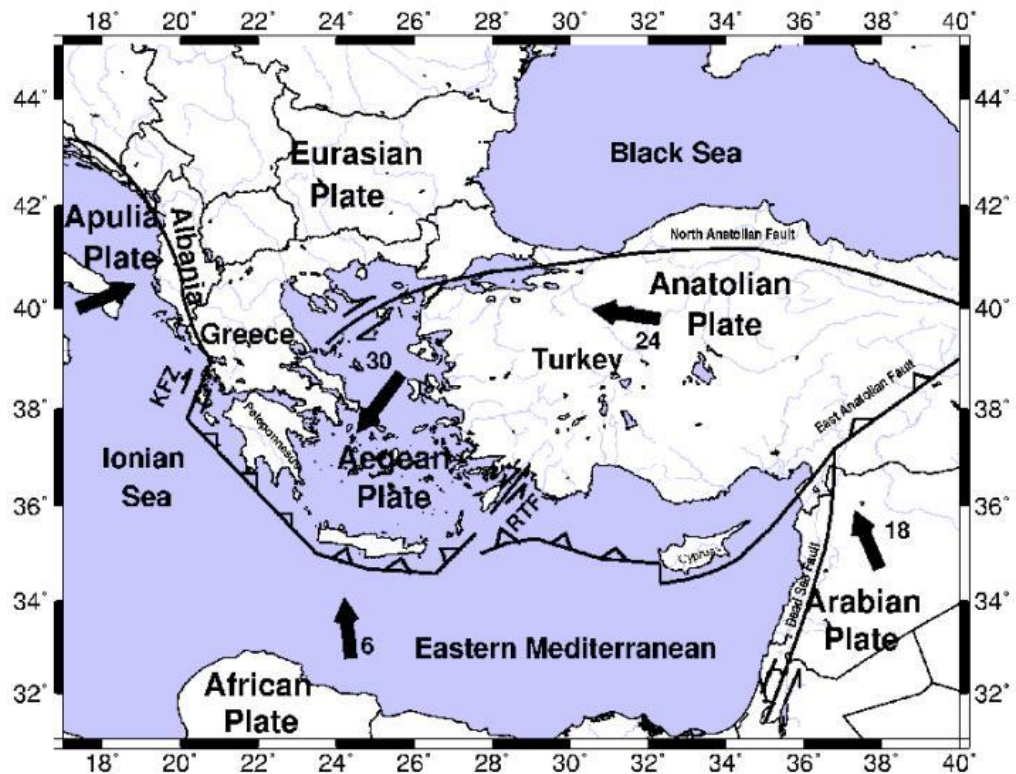
Figure 2.1. Arrows show the plates' direction and the numbers are the velocities (Modified from McClusky 2000)

There is a multi-disciplinary project in literature about the plate interactions through the whole Arabia-Africa and Eurasian plates. Figure 2.2 shows the result of this study which is performed by Reilinger *et al*.,(2006).
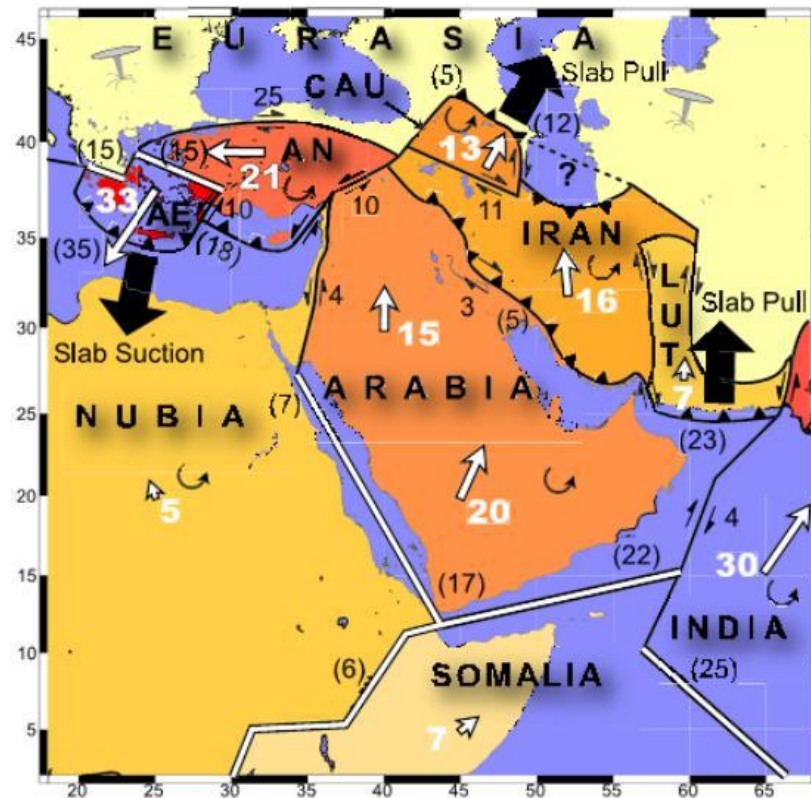
Figure 2.2. CAUC is the Caucasus block, AN is the Anatolian plate and AE is the Aegean plate. Double lines indicate extensional plate boundaries, lines with triangles indicate trust faults and plain lines show strike-slip boundaries. White arrows and adjacent numbers show GPS-derived plate velocities relative to the Eurasia in millimeters per year (Reilinger *et. al.*, 2006)

The Aegean Region has been suffering an active N-S extensional tectonics, under the control of two main motions. One of the motions is the westward escape of the Anatolian plate, bounded by the North Anatolian Fault and East Anatolian Fault, intersecting at the Karliova depression of the East Anatolia with a rate of 20-25 mm/yr. The westward motion changes the direction in the West Anatolia with a rather abrupt counter-clockwise rotation, towards southwest over the Hellenic Trench. The other motion is the N-S extension of the western Anatolia and the Aegean with rate about 30 mm/yr. As a result of these motions a group of E-W trending grabens have been developing. These grabens are bounded by E-W trending normal fault zones which extend about 100-150 km. These fault zones are generally segmented and each segment is no longer than 8-10 km (Yilmaz, 2000).

2.1. Study Area and its Seismicity

The study area is located in western Anatolia, in the Aegean Region. The importance of the study area can be explained by its proximity to the city of İzmir, which is the third most crowded city in Turkey. İzmir is highly populated touristic and commercial center not only for Aegean Region but also for Turkey. The city is also placed with $37^{o}45'$ and $39^{o}15'$ North latitude and $26^{o}15'$ and $28^{o}20'$ East longitude with approximately 12012 km^{2} domain.
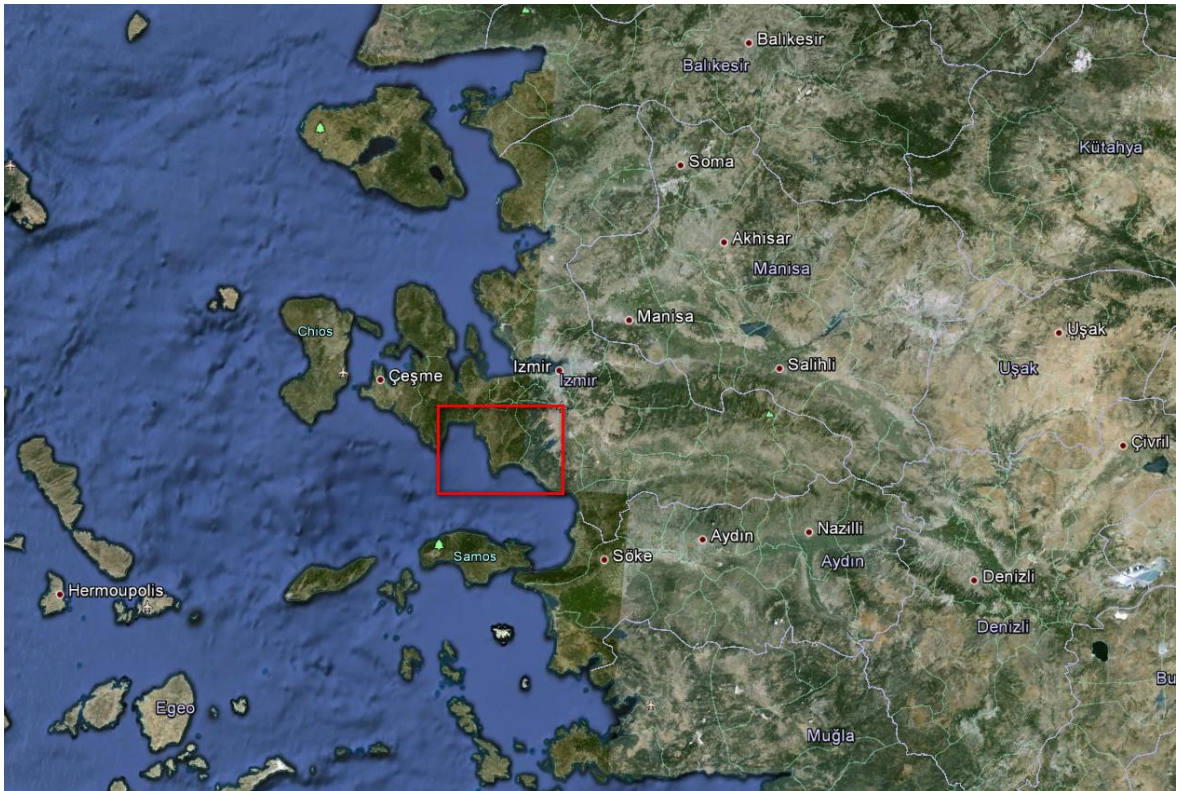
Figure 2.3. Study area and its vicinity

2.2. Active Tectonics of the Study Area

The deformation pattern in the Mediterranean Region which constructs a low elevated part of the Alpine Himalayan belt is rather complex, and usually occurs in continental collision zones. The Aegean Region is bounded to the north by the stable continental Eurasian plate, to the west by the Adriatic Region, to the east by the central Anatolian, and to the south by the oceanic material beneath the Mediterranean Sea which is northern edge of the African plate. Black and Mediterranean Sea floors with mean depth of 1500 and 1300 meters successively, the Aegean Sea floor has a mean depth of 350 m. In other words, the Aegean Sea floor is seen as a high plateau between the deeper Black Sea floor and the Mediterranean Sea floor. The Aegean is characterized by a relatively thicker crust (25-30 km) than a typical oceanic crust, which might be interpreted as a thinned continental crust.

The Aegean is also situated in the convergent boundary between the African plate and Eurasian plate. The African plate has been rotating counter-clockwise with respect to Eurasian plate during the last 92 Ma (Müller *et al*., 1997). The region is also characterized by high heat flow, which is related to thin and deformed (stretched) continental crust. This thinning is still in progress and for this reason, it is the most seismically active and internally deforming area of the entire Alpine-Himalayan belt and at of all continents (Sodoudi, 2005; McKenzie, 1972; Mercier *et al*., 1989; Jackson *et al*., 1994).
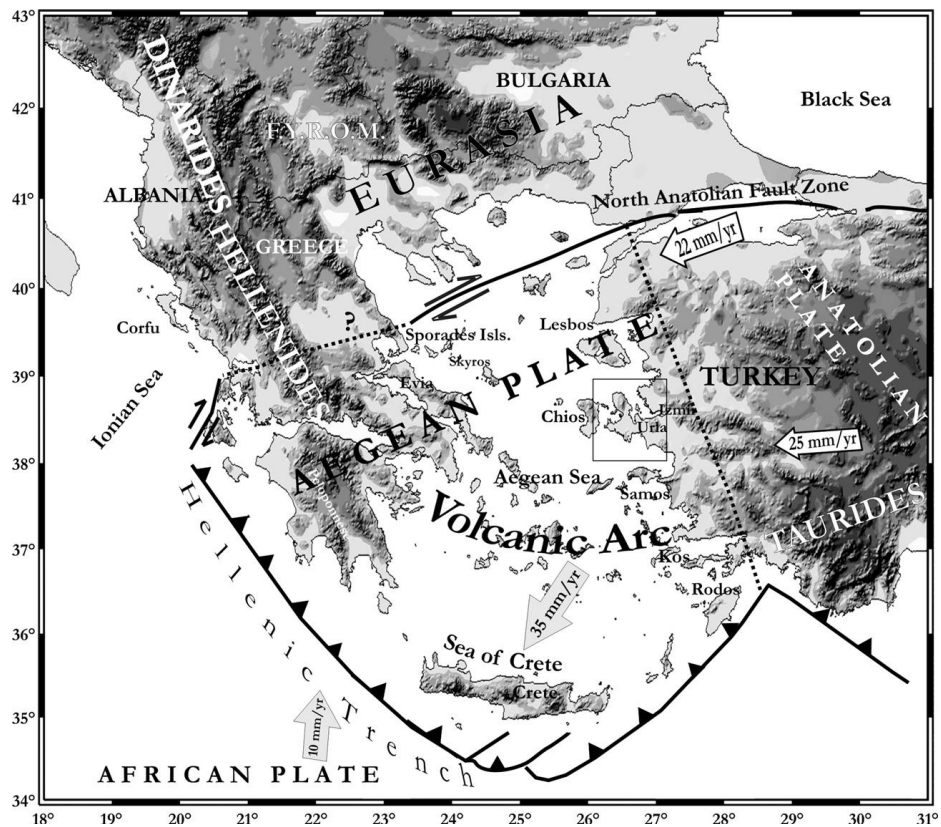
Figure 2.4. Study area tectonics

Figure 2.4 shows the compression and extension zones of the Aegean Region. Papazachos (1999) defines the northern and eastern boundaries of the Aegean plates as dashed lines marked on the figure. The arrows indicate the relative motion with respect to the Eurasian Plate defined by McClusky *et al*. (2000), and the rectangle shows the study area.

The focal mechanism solutions of earthquakes indicate that the faulting in the western part of the Aegean Region is mostly extensional in nature on normal faults, with a NW to WNW strike and slip vectors directed NW to N (Taymaz, 2001). The evidences from paleomagnetism show that this region rotates clockwise relative to the stable Eurasia. Piper *et al*. (2001) indicates, paleomagnetic data in the eastern Aegean Region, is consistent with very small or no rotations in the northern part and possibly counter-clockwise rotations in the south relative to the Europe, including some ambiguities.

The strike-slip faulting that lying through the central Aegean from the east appears to end abruptly in the SW against the NW trending normal faults of Greece (Figure2.4).
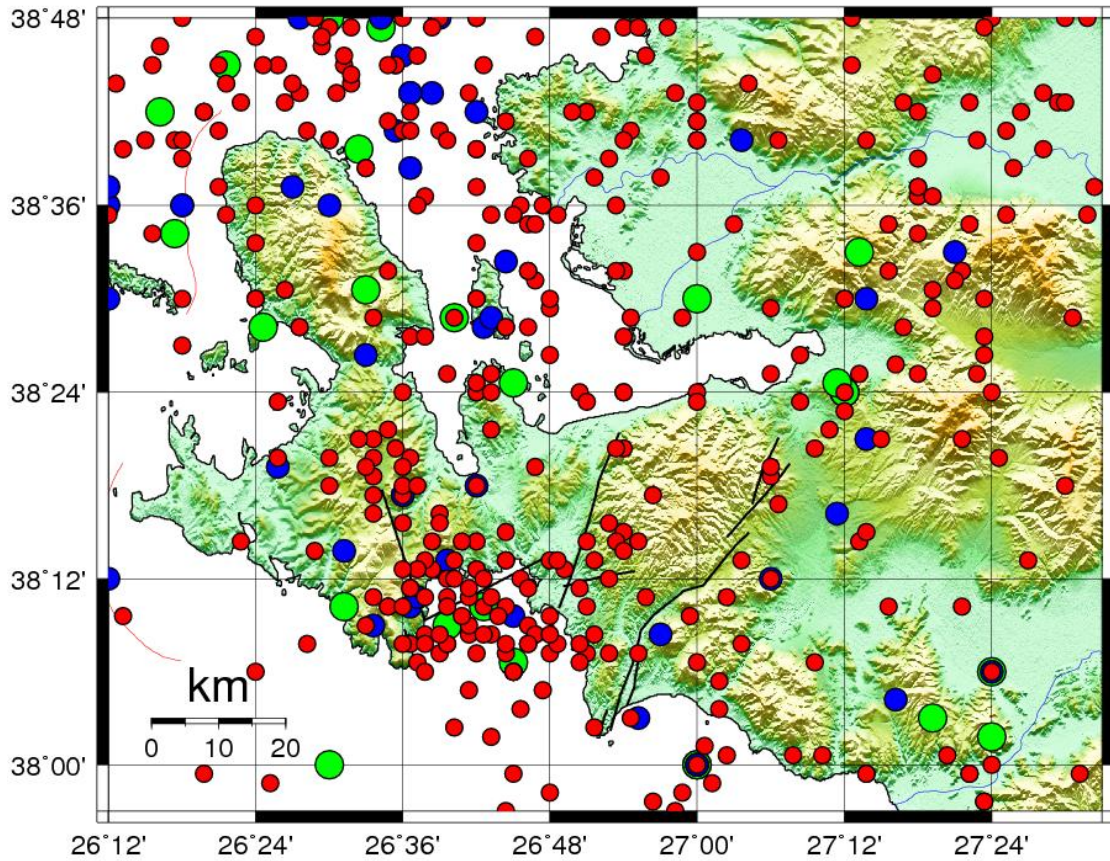
Figure 2.5. 1900-2012 seismicity of the study area

Figure 2.5 shows the earthquakes occurred in the area from 1900 to 2012. Green dots represent the earthquakes M > 5.0. Blue dots represents the earthquakes 4.5 > M > 5.0 and red dots represents the earthquakes 3.5 > M > 4.5. The black lines are the fault lines in the study area (GDMRE Report).

The report on active faults and seismicity in İzmir and its vicinity (Emre *et al*., 2005) by General Directorate of Mineral Research and Exploration (GDMRE) explains 13 active faults approximately 50 km radius area which has a central part of İzmir. These faults are the İzmir fault, the Guzelhisar Fault, the Gulbahce Fault, the Menemen Fault, the

Seferihisar Fault, the Yeni Foca Fault, the Bornova Fault, the Gumuldur Fault, the Gediz Graben Fault zone, the Dagkizilca Fault, the Manisa Fault, the Kemalpasa Fault and the Tuzla Fault (Figure 2.6).
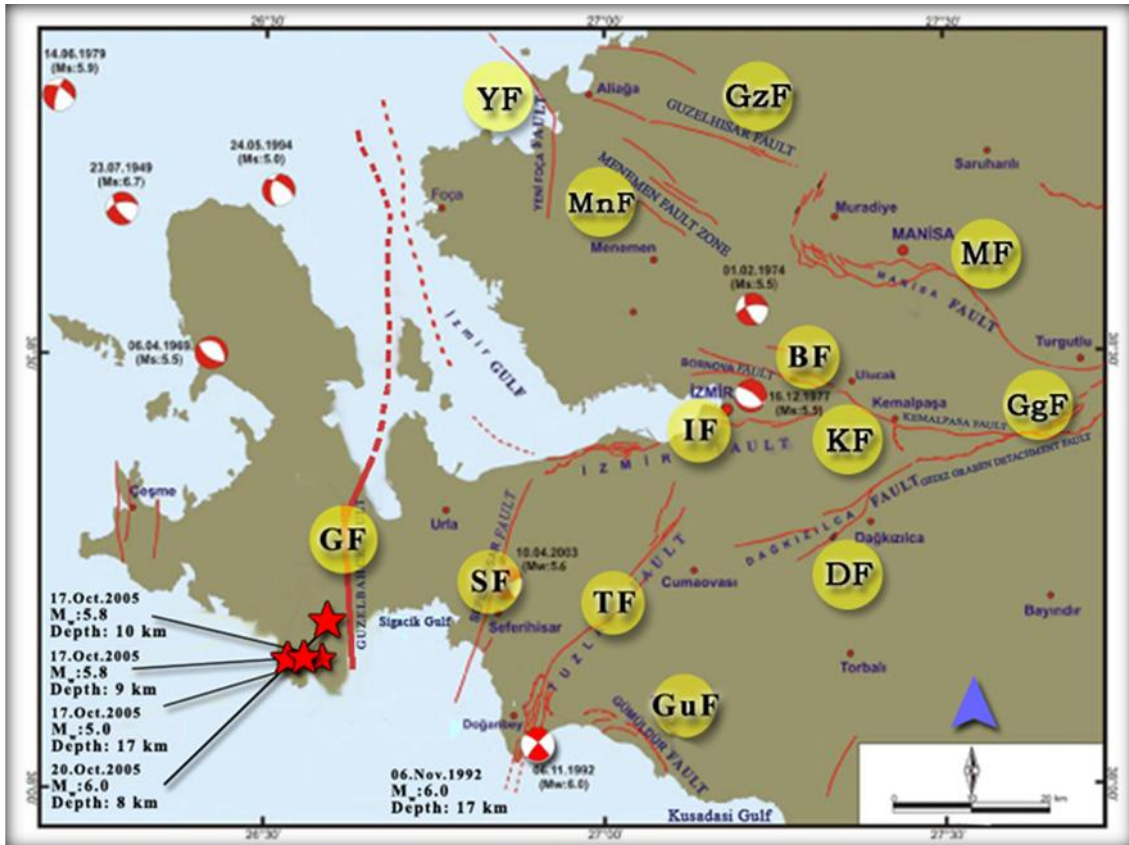
Figure 2.6. Active faults in the study area

The fault lying in the east of the İzmir Gulf is named the İzmir Fault. It is a morphological boundary of that gulf with a lineament of E-W (Emre and Barka, 2000). The İzmir Fault is 35 km long dip-slip normal fault which is lying between Güzelbahçe and Pınarbaşı. The western part of this fault has bifurcated into two segments. Each part of these segments is about 15 km long. GDMRE report indicates that, the İzmir Fault had brought about big earthquakes due to Holocene period with surface ruptures. In addition, geological data indicate that this fault appeared after Miocene.

The Guzelhisar Fault is lying between the province Aliaga and Osmanlica northeast part of İzmir. It is a NW - SE trending fault with 25 km length. The Guzelhisar Fault forms right-lateral strike-slip character. Moreover geomorphologic proof of the Guzelhisar Fault indicates that it was active in the Quaternary period Emre *et al.* (2005) and Saroglu *et al.* (1987).

The Menemen Fault zone resembles the fault cluster which is lying between the Dumanlidag volcano complex and the Gediz lowland. The Menemen Fault Zone has 4 segments which cover an area, 15 km length with NW-SE direction and the width is about 5 km. The longest fault which is in the middle of the fault zone is about 12 km long. According to GDMRE data, these faults are called possibly active faults due to the lack of information and the uncertainty of the Quaternary activity.

The Gülbahçe Fault is separating the Gulf of İzmir and the Karaburun Peninsula in terms of its structural and morphological characteristic. This fault is named the Karaburun Fault (Erdogan, 1990; IESEMP, 2000; GDMRE 2002). However, in order to avoid any misunderstanding in given name, this fault is denoted as the Gülbahçe Fault. Ocakoglu *et al.* (2005) indicates that, this fault is 70 km long with undersea parts. The Gulbahce Fault has two segments, 30 km long in the south part and 40 km long in the north part. In addition, Ocakoglu *et al*. (2005), indicates that the Gulbahce Fault has strike-slip behavior. Moreover, some oblique components can be seen in the north part of this fault.

GDMRE pre assessment report on 17 October 2005 Sığacık, İzmir (Mw=5.6 and Mw=5.9) earthquakes offset locations are densified near the southern part of this fault.

The Yeni Foça Fault is lying between the eastern part of the Nemrut Port and Gerenköy in the south. This is 20 km long N-S lineament trending possibly active fault. The Yeni Foça Fault is interpreting left-lateral strike-slip fault (Altunkaynak and Yilmaz, 2000).

The Bornova Fault cluster is NW-SE lineament trending which is lying northwest of the Gulf of İzmir and south part of Karşıyaka and Kemalpaşa districts. It is an active fault however there is not sufficient data about fault activity.

The Gümüldür Fault is lying between the province Gümüldür and Özdere in the southwest of İzmir. It is about 15 km long with a lineament trending of N55W normal fault. This fault is named as the Ortaköy Fault in Genc *et al.* (2001). The Tuzla Fault is lying along the northwest of this fault. The Gümüldür Fault is a potentially active fault due to the edge of the Gulf of Kuşadası and its effect on the morphology of Quaternary.

The Gediz Graben Fault Zone is, significant fault clusters which are normal fault with E-W trending of this region. The fault clusters consist of 3 main faults. These faults are Dağkızılca, Kemalpaşa and Manisa. The Dağkızılca Fault is bound to the Gediz Graben Fault system. It is a right-lateral strike-slip transfer fault with N70E trending and 27 km long. It is lying between south of Kemalpaşa and Torbalı. The Kemalpaşa Fault is an active fault which is lying between Bağyurdu and Ulucak in the western part of the Gediz Graben (Emre and Barka, 2000). It is 24 km long with a lineament N75E. The Manisa Fault is a normal fault which is located in the northwest branch of the Gediz Graben. It is 40 km long with N65W lineament trending which is lying between Manisa and Turgutlu near Muradiye.

The Tuzla Fault is lying between Gaziemir and Doğanbey in the southwest of İzmir with NE-SW lineament direction (Emre and Barka, 2000). The Tuzla Fault has various names in literature such as the Cumaovası Fault, the Cumalı Reverse Fault and the Orhanlı Fault (Saroglu *et al.*, 1987; Saroglu *et al.*, 1992; Esder 1988; Genc *et al.*, 2001). The fault length is 42 km in the land between Gaziemir and Doğanbey. Ocakoglu *et al.* (2004, 2005) indicates, the Tuzla Fault continues in SW direction and goes beyond 50 km long under the Aegean Sea.

The Tuzla Fault has 3 segments. These are Çatalca, Orhanlı and Cumalı segments. The Çatalca segment is the northeast part of the Tuzla Fault and 15 km long N35E lineament trending. The Çatalca segment is right-lateral strike-slip fault according to the Quaternary geomorphologic data (Ozener H., *et al.*, 2012). The Orhanlı segment has N50E lineament trending with 16 km long fault which is located in the southeast of the Tuzla Fault. The last part of the Tuzla Fault is the Cumalı segment. The Cumalı segment forms a fault zone, in which faults are parallel to each other in NNE-SSW direction in the southwest part of the Tuzla Fault. The Cumalı Fault Zone is lying between Doğanbey Cape and Cumalı thermal springs with 15 km long. This segment also goes beyond 25 km with submarine (Ocakoglu *et al*., 2005).

The Tuzla Fault is well recognized by recent earthquakes Mw= 6.0 which was occurred on the Doğanbey promontory. Though the morphology at the Doğanbey promontory is seen left lateral, the focal mechanism solutions indicate that the Tuzla Fault character is right lateral (Tan and Taymaz, 2001). Moreover, geological observations reveal a right lateral offset of 200-700 meters at young river beds of Holocene age along the Tuzla Fault (Emre and Barka, 2000; Ocakoglu, 2004).

Table 2.1. Earthquakes occurred in the area in 20 years M > 4.5 (KOERI – NEMC)

Date	Latitude (deg)	Longitude (deg)	Magnitude (M)	Depth (km)
06 November 1992	38.16	26.99	5.7	17.00
06 November 1992	38.03	27.06	4.5	10.00
28 January 1994	38.69	27.49	5.2	5.00
24 May 1994	38.66	26.54	5.0	17.00
24 May 1994	38.76	26.60	5.0	16.00
24 May 1994	38.68	26.48	4.8	14.00
03 February 1996	37.79	26.87	4.5	22.00
02 April 1996	37.78	26.64	4.9	12.00
09 July 1998	37.95	26.74	5.3	21.00
21 January 2002	38.68	27.83	4.7	10.66
23 May 2002	38.76	26.43	4.6	14.41
10 April 2003	38.22	26.80	5.6	12.19
17 April 2003	38.22	26.94	4.8	15.23
16 December 2003	38.97	26.83	4.6	15.60
24 March 2004	38.91	26.74	4.8	16.13
05 November 2004	39.18	27.76	4.5	8.81
17 October 2005	38.17	26.58	5.7	10.80
17 October 2005	38.18	26.62	4.5	14.40
17 October 2005	38.13	26.55	4.7	15.20
17 October 2005	38.17	26.53	5.8	10.50
17 October 2005	38.14	26.62	5.2	20.70
19 October 2005	38.16	26.69	4.6	12.30
20 October 2005	38.17	26.58	5.9	7.50
29 October 2005	38.10	26.64	4.5	14.20
31 October 2005	38.16	26.59	4.8	8.40
24 December 2005	38.81	27.76	4.6	17.00
12 January 2008	38.92	26.08	4.8	9.10
20 June 2009	37.65	26.75	5.0	9.90
26 March 2010	38.14	26.22	4.7	9.20
11 November 2010	37.92	27.35	4.8	14.10
05 December 2011	38.82	26.27	5.1	7.20

3. GLOBAL POSITIONING SYSTEM

3.1. Use of GPS in Tectonic Studies

GPS is a common geodetic method in tectonic studies. The advantages which make this method that common is its independency from weather conditions, higher precision and accuracy, a smaller budget than any other geodetic method and its portability (Cakmak, 2010).

Use of GPS in tectonic studies began in Turkey in 1988. Pre-seismic phase is the time period before a large earthquake. The studies carried out before 1999 Izmit Earthquake are the pre-seismic studies. Pre seismic studies are carried out by many institutions from Turkey and abroad such as KOERI, ITU, TUBITAK, General Command of Mapping, MIT, ETH Zurich *etc.* (Cakmak,2010).

Co-seismic phase is the time of a large earthquake. Data from continuous stations and campaign surveys help us to determine the displacements in both horizontal and vertical directions. There is a relation between the amount of displacement caused by an earthquake and its magnitude.

Post-seismic phase is the time period after a large earthquake. A fault that has experienced a significant rupture often continues to accommodate significant slip after the rupture. This period can be defined as the fault's last phase before the interseismic phase which is a steady time period and usually defined as the time period between two large earthquakes. Post-seismic phase can be observed by using GPS and velocity of the fault can be determined precisely.

GPS is used in every phase of the tectonic studies and is a useful tool for scientists to understand the characteristics of tectonics in an area. GPS is being used in a global scale

lately. Global velocity and strain maps are created and more continuous stations are as realized as arrays.

3.1.1. Error Sources of GPS

Even though GPS is the most advanced and precise technology developed until now, it has some drawbacks as well as the other systems. In other words, GPS observation results are affected by errors and biases. These errors and biases are negligible in general use like navigation or military applications but in scientific applications such as, precise point positioning, investigation of plate tectonics *etc.*, these errors and biases must be modeled and taken into account during the process of the data (Kahveci, 2009).

Satellite ranging is the main concept of GPS, and error sources effecting on this concept are :

- Ephemeris data

Ephemeris errors result when the GPS message does not transmit the correct satellite location.

- Satellite clock - Errors in the transmitted clock

Fundamental to GPS is the one-way ranging that ultimately depends on satellite clock predictability. The satellite's atomic clocks experience noise and clock drift errors.

- Ionosphere

Because of free electrons in the ionosphere, GPS signals do not travel at the vacuum speed of light as they transit this region. This causes errors in the corrections of pseudorange.

- Troposphere

Another deviation from the vacuum speed of light is caused by the troposphere. Variations in temperature, pressure, and humidity all contribute to variations in the speed of light of radio waves.

- Multipath

Multipath is the error caused by reflected signals entering the receiver antenna.

- Receiver

Errors in the receiver's measurement of range caused by thermal noise, software accuracy, and inter-channel biases ("GPS Error Analysis", pages 478-483, Global Positioning System: Theory and Applications by Bradford W. Parkinson, James J. Spilker Jr. Eds.).

3.1.2. GPS Surveying Methods

There are various methods for GPS surveying. The method should be chosen by considering survey objectives, desired precision, available equipment and logistics. In scientific applications of GPS, high precision is desired which requires a rigorous field methodology and longer occupation times. Table 3.1 shows the features of most common surveying methods.

Table 3.1. Features of most common surveying methods

Survey style	Typical accuracy	Occupation time	Typical applications
Continuous	< 0.5 cm	Months or more	Crustal deformation, geophysics, reference stations
Static	0.5 cm – 2.5 cm	Hours to days	Crustal deformation, geodetic control, very long baseline surveys, geophysics
Rapid Static	1 cm – 3 cm	Minutes	Short baseline surveys, glaciology
Kinematic (post-processing and real-time)	1 cm – 5 cm	Seconds	Short baselines, closely spaced points, vehicle positioning, feature surveys, GIS, mapping, and navigation (RTK only)

3.2. GPS Campaigns in the Study Area

Geodesy Department of KOERI at Boğaziçi University began studying the Tuzla Fault in 2009 by using GPS method. First of all reconnaissance has been performed in the study area in order to establish the GPS sites by taking into account different parameters such as distance to the fault, rock types and GPS requirements (Figure 3.1). From the reconnaissance to the analysis of data collected, including observation, planning and measurement method, each step of GPS campaigns has basic importance in GPS applications.
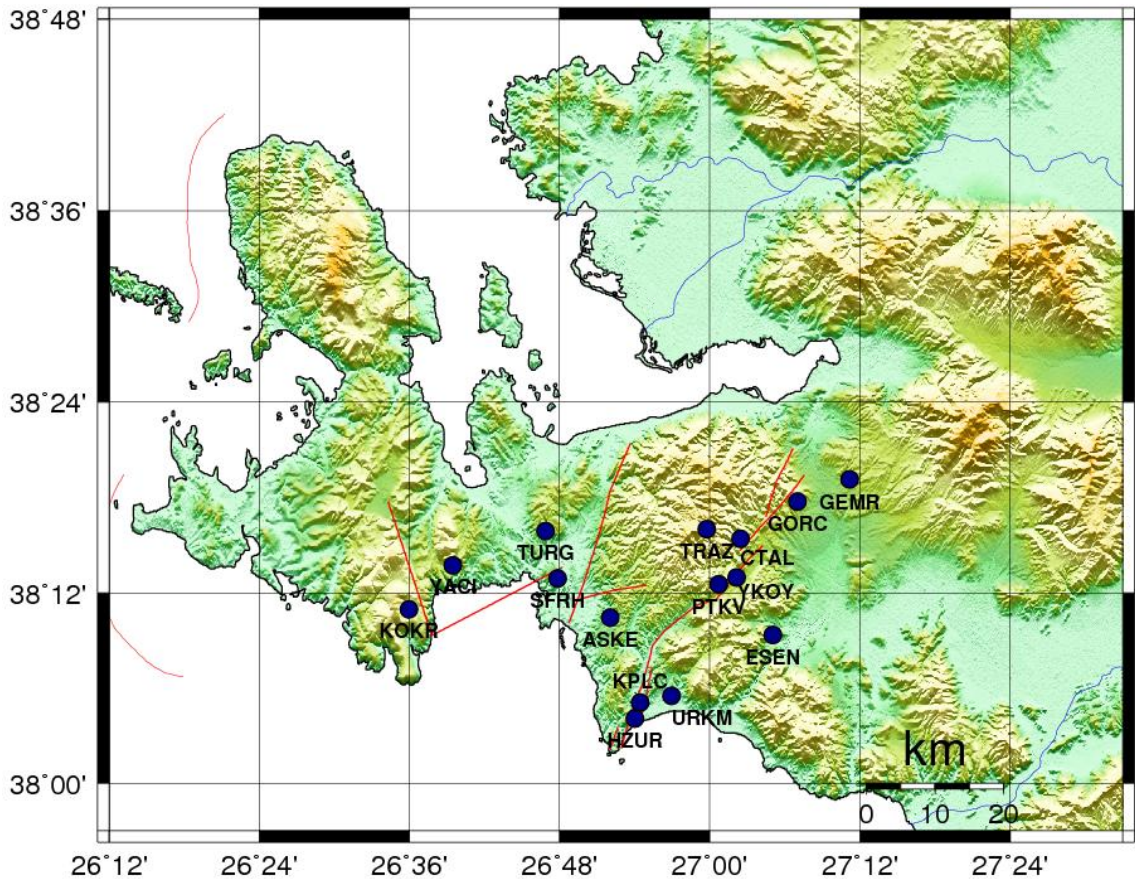
Figure 3.1. GPS stations in the study area

GPS sites were established in optimum number and gradually in distance 1, 2, and 6 km away from active faults. GPS sites were required not to be affected by surface movement such as landslide and transportation possibilities and the owners of the lands were also considered. GPS sites were placed into bedrock using high quality geodetic monuments. Selection of session lengths, receiver and antenna distribution are necessary in order to avoid the systematic biases (Ozener, 2010). The coordinates and names of the GPS stations are given in Table 3.2.

Table 3.2. Coordinates of GPS stations

Station	Station ID	Latitude^o(E) WGS - 84	Longitude^o(N) WGS - 84
Askeriye	ASKE	38° 10' 27″	26° 51' 60″
Çatalca	CTAL	38° 15' 26″	27° 02' 29″
Esenli	ESEN	38° 09' 21″	27° 05' 01″
Gaziemir	GEMR	38° 19' 08″	27° 11' 09″
Görece	GORC	38° 17' 45″	27° 06' 60″
Huzur Sitesi	HZUR	38° 04' 04″	26° 54' 01″
Kokar	KOKR	38° 10' 59″	26° 35' 58″
Kaplıca	KPLC	38° 05' 07″	26° 54' 27″
Petek Vadisi	PTKV	38° 12' 33″	27° 00' 45″
Seferihisar	SFRH	38° 12' 56″	26° 47' 50″
Tırazlı	TRAZ	38° 16' 04″	26° 59' 34″
Turgutlu	TURG	38° 15' 54″	26° 46' 53″
Ürkmez	URKM	38° 05' 33″	26° 56' 55″
Yağcılar	YACI	38° 13' 45″	26° 39' 28″
Yeniköy	YKOY	38° 12' 57″	27° 02' 10″

Five GPS campaigns have been carried out in the study area since 2009. The sub – cm precision is desired in crustal deformation studies. For this purpose, GPS campaigns are carried out as 10 hour/day for each station. Campaign observations are planned to be completed in 2 days and common stations are chosen to be observed in both sessions to increase repeatability.

Trimble 4000 SSI, Trimble 4000 SSE and Trimble 5700 receivers are used during the measurements and Permanent L1\L2, Compact L1\L2 and Zephyr Geodetic antennas are used with the receivers.

Figure 3.2. A view from site ESEN

Table 3.3. GPS campaign dates and observation duration

YEAR	Day of Year	Observation Duration	Elevation mask (deg)	Data Rate (sec)
2009	229-230	10h	10	15
2010	152-153	10h	10	15
2011	145-146	10h	10	15
2012	038-039	10h	10	15
2012	157-158	10h	10	15

3.3. GPS Data Analysis

3.3.1. GPS Data Analyzing Software

In GPS data processing, two types of software are used; commercial and scientific. Commercial software is used in common engineering applications and various types of GPS data collected by any surveying method can be processed. Scientific software is generally used in crustal deformation studies but any kind of study which requires GPS data processing can be carried out by scientific software. A list of scientific software and its supporting institution is given in Table 3.4.

Table 3.4. Scientific GPS data processing software and supporting institutions

Software	Institute
Bernese	AIUB
GAMIT/GLOBK	MIT-SIO
GIPSY/OASIS II	JPL(NASA)
PAGE5	NOAA
GEONAP	University of Hannover
MURO.COSM	University of Texas – Van Martin System
DIPOP	University of New Brunswick

GAMIT/GLOBK (Herring *et al.*, 2010a) software is chosen in this study for data process. The software works under two main modules. First module is GAMIT and it consists of various programs to process GPS data and results return as the position estimates. The second main module is GLOBK which is a Kalman filter whose primary purpose is to combine various geodetic solutions from the processing of primary data from space geodetic or terrestrial observations.

The main GAMIT modules require seven types of input:

• Raw phase and pseudo-range data in the form of ASCII X-files (one for each station within each session)

• Station coordinates in the form of an L-file

• Receiver and antenna information for each site (file station.info)

• Satellite list and scenario (file session.info)

• Initial conditions for the satellites' orbits in a G-file (or a tabulated ephemeris in a T-file)

• Satellite and station clock values (I-, J-, and K-files)

• Control files for the analysis (sestbl. and sittbl.)

•"Standard" tables to provide lunar/solar ephemerides, the Earth's rotation, geodetic datums, and spacecraft and instrumentation information. (Herring *et. al.*, 2010b).

GLOBK accepts as data, or "quasi-observations" the estimates and associated covariance matrices for station coordinates, earth-rotation parameters, orbital parameters, and source positions generated from analyses of the primary observations. These primary solutions should be performed with loose a priori uncertainties assigned to the global parameters, so that constraints can be applied uniformly in the combined solution. Although GLOBK has been developed as an interface with GAMIT (for GPS) and CALC/SOLVE (for VLBI), there is little intrinsic to this pairing in its structure. GLOBK can be used to combine solution files generated by other GPS software (*e.g.* Bernese and GIPSY), as well as for terrestrial and SLR observations.

There are three common modes, or applications, in which GLBOK is used:

1. Combination of individual sessions (*e.g.*, days) of observations to obtain an estimate of station coordinates averaged over a multi-day experiment. For GPS analyses, orbital parameters can be treated as stochastic, allowing either short- or long-arc solutions.

2. Combination of experiment-averaged estimates of station coordinates obtained from several years of observations to estimate station velocities.

3. Independent estimation of coordinates from individual sessions or experiments to generate time series assessment of measurement precision over days (session combination) or years (experiment combination). (Herring *et. al.,* 2010c).

3.3.2. GPS Data Analyzing Strategies

Data analyzing strategy is the first step to begin processing. Selection of the models and parameters are important as they have direct effect on the process results.

- Each campaign was processed using the International Terrestrial Reference Frame ITRF_2005.

- Precise final orbits by the International GNSS Service (IGS) were obtained in SP3 (Standard Product 3) format from SOPAC (Scripps Orbit and Permanent Array Center).

- Earth Rotation Parameters (ERP) came from USNO_bull_b (United States Naval Observatory_bulletin_b).

- 15 stations from IGS global monitoring network were included in the process. These IGS stations are TUBI, TRAB, ORID, ANKR, BUCU, ISTA, GRAZ, KIT3, MATE, NICO, NSSP, ONSA, SOFI, WTZR, ZECK.

- The 9-parameter Berne model was used for the effects of radiation and the pressure.

- Scherneck model was used for the solid earth tide and the ocean tide loading effects.

- Zenith Delay unknowns were computed based on the Saastamoinen a priori standard troposphere model with 2-h intervals.

- Iono-free LC (L3) linear combination of L1 and L2 carrier phases was used.

- The model, which depended on the height, was preferred for the phase centers of the antennas.

- Loosely constrained daily solutions obtained from GAMIT were included in the ITRF_2005 reference frame by a 7 parameters (3 offset−3 rotation−1 scale) transformation with 15 global IGS stations.

## 3.4. GPS Data Processing Results

GPS surveying campaigns' data is processed in GAMIT/GLOBK software. Horizontal GPS velocities in Eurasia-fixed frame and 1-sigma uncertainties plotted with 95 percent confidence ellipses (Figure 3.3). The velocities determined by using the data of five campaigns between 2009 and 2012 are given in Table 3.5. Campaign data for HZUR site in 38th day of 2012 was excluded in process. The time series of the sites (Appendix) are examined and a blunder was found in the horizontal components of HZUR site.
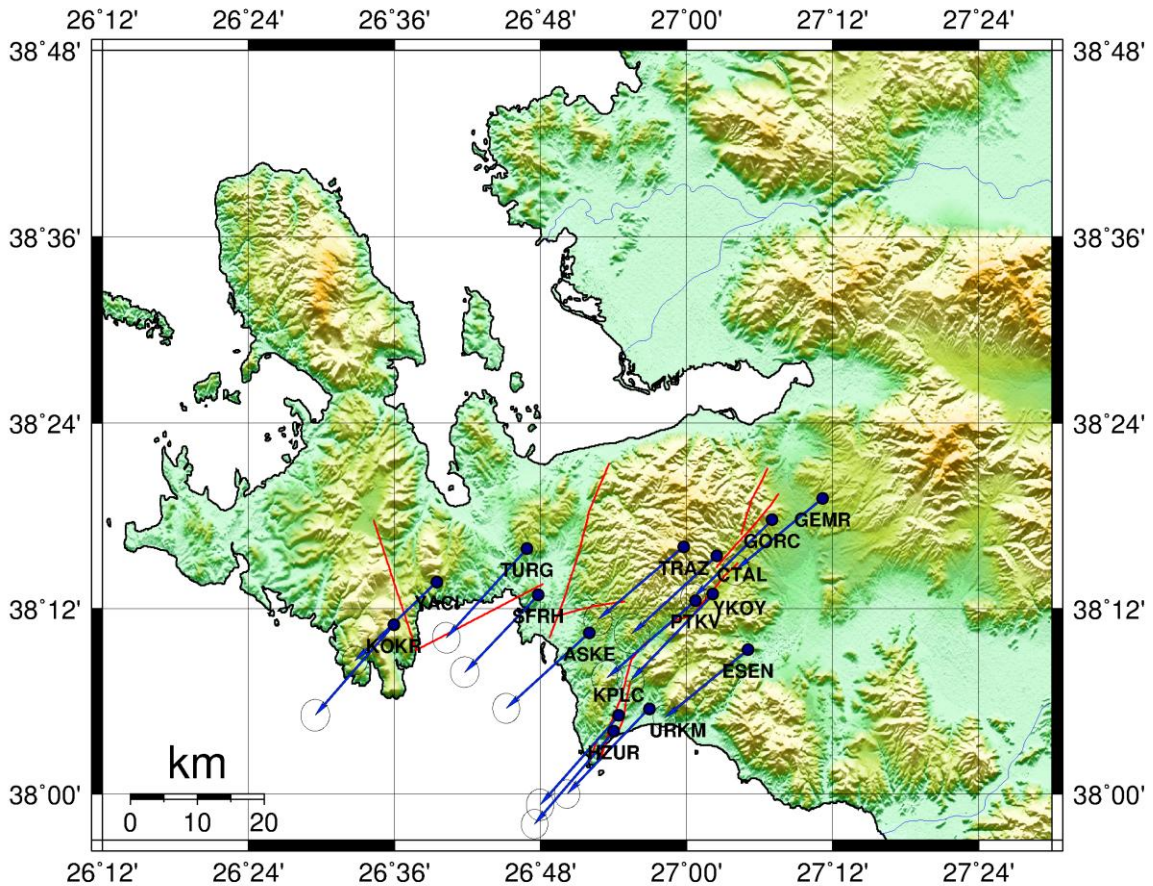
Figure 3.3. Horizontal GPS velocities in Eurasia-fixed frame and 1-sigma uncertainties plotted with 95 percent confidence ellipses

Table 3.5. Summary of velocity estimates in Eurasia fixed frame

Site	Latitude (deg)	Longitude (deg)	Evel (mm/yr)	Nvel (mm/yr)	Esig (mm/yr)	Nsig (mm/yr)	RHO
GEMR	38.31893	27.18589	-20.32	-16.69	1.45	1.30	0.031
GORC	38.29572	27.11659	-18.43	-18.16	1.33	1.19	0.005
ESEN	38.15567	27.08366	-19.44	-15.88	1.22	1.11	-0.044
CTAL	38.25710	27.04138	-19.89	-18.20	1.90	1.70	-0.014
YKOY	38.21573	27.03605	-19.32	-20.11	1.42	1.32	-0.084
PTKV	38.20897	27.01246	-20.75	-18.05	1.62	1.48	-0.006
TRAZ	38.26691	26.99559	-20.00	-17.00	1.52	1.35	0.010
URKM	38.09247	26.94867	-19.23	-20.03	1.36	1.22	0.008
KPLC	38.08517	26.90745	-18.50	-20.94	1.51	1.31	-0.004
HZUR	38.06769	26.90042	-18.58	-21.67	1.40	1.27	0.016
ASKE	38.17417	26.86663	-19.45	-17.66	1.43	1.29	-0.008
SFRH	38.21542	26.79729	-17.31	-18.15	1.46	1.36	0.013
TURG	38.26488	26.78140	-18.88	-20.83	1.47	1.32	-0.031
YACI	38.22923	26.65781	-19.18	-18.46	1.38	1.22	0.027
KOKR	38.18291	26.59937	-18.45	-21.17	1.51	1.38	0.007

4. STRESS AND STRAIN

4.1. Stress

Stress can be defined as acting force per unit area. It has the same units as pressure but also has a direction. However, stress is a much more complex quantity than pressure because it varies both with direction and with the surface it acts on. There are three types of stress: compression, tension, and shear (Figure 4.1). If stress is not equal from all directions, it is said that the stress is a differential stress.
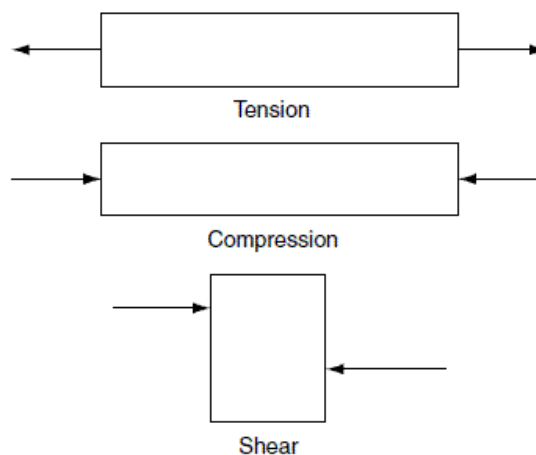
Figure 4.1. Types of stress

Tensional stress is the stress which stretches the object. Compressional stress is the stress which squeezes the object and shear stress is the stress which results in slippage and translation. (http://www.tulane.edu/~sanelson/geol111/deform.htm)

Stress is not directly measurable. It is important to know the stress situation for reconstructing and estimating tectonic regimes, and for assessing fault kinematics. It is generally assumed that, in the plate-tectonic framework, large scale deformations occur

due to local response of the lithosphere to induced stresses. Understanding the origin and distinguishing the different types of stress, as well as knowing its orientation and magnitude is therefore a crucial tool in analyzing and understanding tectonic deformation (Arslan,2007).

4.2. Strain

Tectonic plates slide past, over and apart from each other along fault lines. This movement causes rocks to be subject to a massive force. The force per unit area is called stress. Rocks respond to stress differently depending on the pressure and temperature (depth in Earth) and mineralogical composition of the rock. Strain is defined as the amount of deformation an object experiences compared to its original size and shape. Strain is the deformation of the rock as a response to the stress.

Strain is very much related with displacement. If the term strain wanted to be explained by using coordinates, it is the rate of coordinate differences to the original coordinates. Strain can be calculated by linear transformation, using GPS velocities along the fault planes. In addition, GPS is an important tool to calculate strain rates of areas where assumed to have potential to generate earthquakes (Jackson *et al.*,1999). Strain is also known as normal unit deformation as it is basically a rate expressed without unit.

4.3. Relationship Between Stress and Strain

The reaction of rocks to an imposed stress depends on the material, temperature and pressure. When stress starts to affect a rock, it is deformed until it reaches its yield point. The deformation can be recovered if stress is removed before it reaches its yield point. This is called elastic deformation. If the stress exceeds the yield point the deformation cannot be recovered and this is called plastic deformation. If the stress continues to grow, the rock will eventually fracture and this is called brittle failure (Figure 4.2). Brittle failure may occur if stress is imposed suddenly as well (Arslan, 2007).
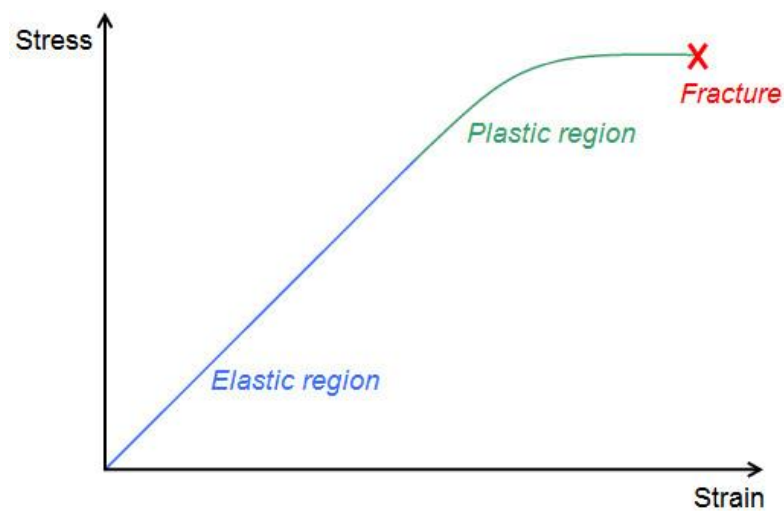
Figure 4.2. Stages of deformation

4.4. Calculation of Strain Parameters in Two-Dimensions

Positions of P and Q points, which are on a deforming plate with differential distance(dx_i) to each other, are shown in Figure 4.3 (Demir, 1999).
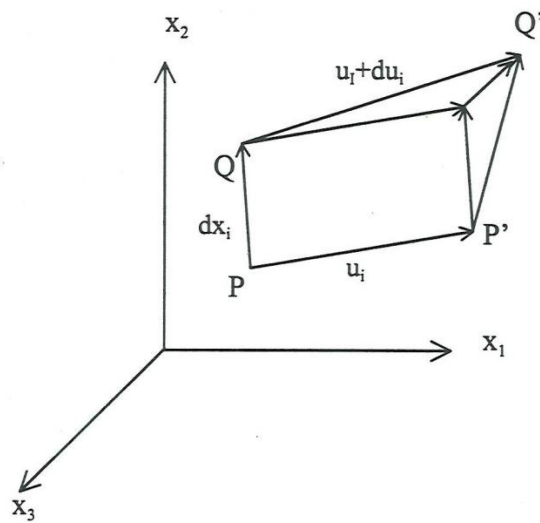
Figure 4.3. Positions of P and Q points before and after deformation

Relationship between P and Q points' positions before and after the deformation is,

$$P\,(x_i) \rightarrow P'(x_i + u_i)$$

$$\text{(4.1)}$$

$$Q\,(x_i) \rightarrow Q'(x_i + dx_i + u_i + du_i) \quad (i = 1,2,3)$$

If it is assumed that, the deformation is homogenous and continuous and the first derivatives of the deformation is continuous and too small, general equation is,

$$u_i = u_i(x_1, x_2, x_3)$$

<div align="right">(4.2)</div>

By using the chain rule, relative displacements of point positions (du_i),

$$du_i = \frac{\partial u_i}{\partial x_1} dx_1 + \frac{\partial u_i}{\partial x_2} dx_2 + \frac{\partial u_i}{\partial x_3} dx_3 \qquad (i = 1,2,3)$$

<div align="right">(4.3a)</div>

or by using Einstein summation convention (Mase, 1970)

$$du_i = \frac{\partial u_i}{\partial x_j} dx_j \qquad (j = 1,2,3), (i = 1,2,3)$$

<div align="right">(4.3b)</div>

In this equation $\partial u_i / \partial x_j$ is the 2nd degree velocity gradient tensor of two vectors and dx_j is the position differences. If we integrate both sides of the equation, in other words if we assume one of the points is in the center of the coordinate system and stable, u_i velocities at points,

$$u_i = \frac{\partial u_i}{\partial x_j} dx_j + t_i \qquad (j = 1,2,3), (i = 1,2,3)$$

<div align="right">(4.4)</div>

In Equation (4.4) t_i denotes translation (rigid block movements) of the points. If the displacement of the points is relative to each other ti disappears as in (4.3b). If Equation (4.4) is written down in open form,

$$\begin{bmatrix} u_1 \\ u_2 \\ u_3 \end{bmatrix} = \begin{bmatrix} \dfrac{\partial u_1}{\partial x_1} & \dfrac{\partial u_1}{\partial x_2} & \dfrac{\partial u_1}{\partial x_3} \\ \dfrac{\partial u_2}{\partial x_1} & \dfrac{\partial u_2}{\partial x_2} & \dfrac{\partial u_2}{\partial x_2} \\ \dfrac{\partial u_3}{\partial x_1} & \dfrac{\partial u_3}{\partial x_2} & \dfrac{\partial u_3}{\partial x_3} \end{bmatrix} \begin{bmatrix} x_1 \\ x_2 \\ x_3 \end{bmatrix} + \begin{bmatrix} t_1 \\ t_2 \\ t_3 \end{bmatrix}$$

(4.5)

or

$$u = Lx + t \qquad (4.6)$$

Relative displacements,

$$du = L\,dx \qquad (4.7)$$

Velocity gradient tensor L can be denoted as the summation of symmetric and anti-symmetric of two matrices,

$$L = E + R \qquad (4.8)$$

E is the symmetric strain tensor and R is the anti-symmetric rotation tensor.

$$E = \begin{bmatrix} e_{11} & e_{12} & e_{13} \\ e_{21} & e_{22} & e_{23} \\ e_{31} & e_{32} & e_{33} \end{bmatrix} = \begin{bmatrix} \partial u_1/\partial x_1 & \frac{1}{2}(\partial u_1/\partial x_2 + \partial u_2/\partial x_1) & \frac{1}{2}(\partial u_1/\partial x_3 + \partial u_3/\partial x_1) \\ & \partial u_2/\partial x_2 & \frac{1}{2}(\partial u_2/\partial x_3 + \partial u_3/\partial x_2) \\ \text{Symmetric} & & \partial u_3/\partial x_3 \end{bmatrix} \quad (4.9)$$

$$R=\begin{bmatrix} 0 & -\omega_{12} & \omega_{13} \\ \omega_{12} & 0 & -\omega_{23} \\ -\omega_{13} & \omega_{23} & 0 \end{bmatrix}=\begin{bmatrix} 0 & -\frac{1}{2}(\partial u_1/\partial x_2 - \partial u_2/\partial x_1) & \frac{1}{2}(\partial u_1/\partial x_3 - \partial u_3/\partial x_1) \\ \omega_{12} & 0 & -\frac{1}{2}(\partial u_2/\partial x_3 - \partial u_3/\partial x_2) \\ -\omega_{13} & \omega_{23} & 0 \end{bmatrix} \quad (4.10)$$

Elements of E and R matrices can be denoted as

$$e_{ii} = \frac{\partial u_i}{\partial_i}, \qquad e_{ij} = \frac{1}{2}(\partial u_i/\partial x_j + \partial u_j/\partial x_i)$$

$$(4.11)$$

$$\omega_{ii} = 0, \qquad \omega_{ii} = \frac{1}{2}(\partial u_1/\partial x_2 - \partial u_2/\partial x_1)$$

Diagonal elements (e_{ii}) of strain tensor E, denotes deformation in unit length along coordinate axes and the other elements (e_{ij}) denotes angular deformation with respect to coordinate axes and is free from translation.

Elements of rotation tensor R, denotes differential rotation of the rigid body which is on the plane defined by the coordinate axes. If the Equation (4.6) which denotes the linear relation between strain field and velocity field is rewritten,

$$u = (E+R) x + t \quad (4.12)$$

It shows that factors on displacement originate from strain tensor by E x, rotation tensor by R x and translation t. According to this, movement of a mass is equal to

summation of translation, rotation and strain components. Even though there is no need for a reference system to measure strain caused by relative movements within the mass, it is mandatory to have reference system for translation and rotation.

Coordinate axes are denoted as x (east) and y (north) in general use instead of 1 and 2 and two dimensional strain tensor is taken into account as,

$$E = \begin{bmatrix} e_{xx} & e_{xy} \\ e_{xy} & e_{yy} \end{bmatrix}$$

(4.13)

So the strain parameters are denoted by the equations below (Jeager, 1969; Prescott et al., 1979; Mierlo, 1981; Welsch, 1981) :

Dilatation	$\Delta = e_{xx} + e_{yy}$	(4.14)
Pure Shear	$\gamma_1 = e_{xx} - e_{yy}$	(4.15)
Engineering Shear	$\gamma_2 = 2\, e_{xy}$	(4.16)
Shear Strain	$\gamma = (\gamma_1^2 + \gamma_2^2)^{1/2}$	(4.17)
Maximum Principal Strain	$\varepsilon_1 = 1/2\, (\Delta + \gamma)$	(4.18)
Minimum Principal Strain	$\varepsilon_2 = 1/2\, (\Delta - \gamma)$	(4.19)
Maximum Strain Direction (Azimuth)	$\varphi = 1/2\, \text{atan}\,(\gamma_2 / \gamma_1)$	(4.20)
Shear Strain Direction	$\psi = \varphi + \pi/4$	(4.21)

If the strain field is homogenous, points on a circle before deformation are going to be on an ellipse after deformation which is called strain ellipse (Figure 4.4) (Demir, 1999).
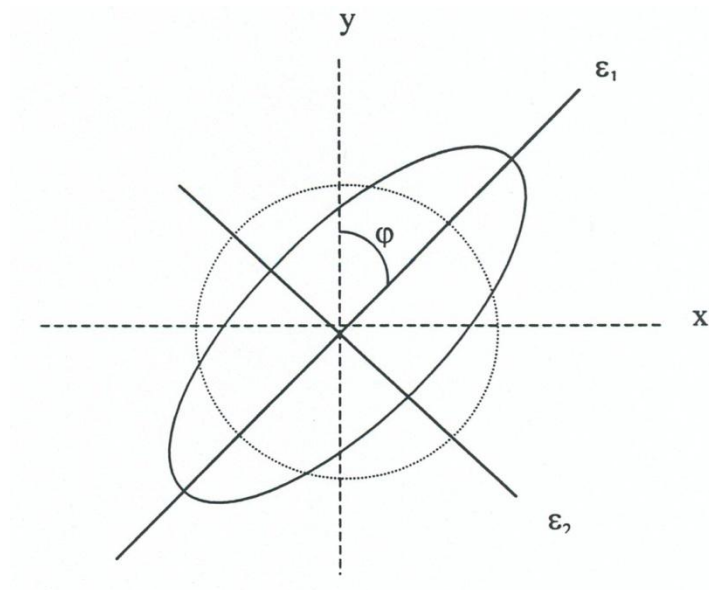
Figure 4.4. Strain ellipse and maximum, minimum principal strain parameters

Maximum and minimum principal strain parameters might be positive or negative. Positive values indicate extension and negative values indicate compression in the given direction. If maximum and minimum principal strain parameters are positive, unit circle is defined by the strain ellipse. In case of one parameter being positive and the other is negative, it is a hyperbola and if both parameters are negative, it is a virtual circle (Vanicek *et al.*, 1981).

4.5. Strain Analysis with Geodetic Methods

Strain analysis is commonly used in determining the deformation of an object. Determining and monitoring of strain accumulation can be performed by geodetic methods. Main geodetic methods used in strain analysis are,

- Measurement or adjusted measurement differences that are; length, angle and azimuth differences

- Coordinate differences
- Determination of strain parameters in an adjustment model

Either of these methods are advantageous or disadvantageous according to the need of concerned problem. For the determination of these requirements, the strain parameters' values and their accuracy have great importance. Table 4.1 indicates the strain parameters that can be determined by which geodetic measurement method (Demir,1999).

Table 4.1. Strain parameters that are defined by repeated geodetic observations

Parameters	Length	Azimuth	Angle	GPS
Dilatation (Δ)	+			+
Shear Strain (γ)	+	+	+	+
Principal Strains ($\varepsilon_1, \varepsilon_2$)	+			+
Rotation Angle (φ)	+	+	+	+
Angular Strain (ω)		+		+

The results below can be inferred from Table 4.1 :

- Angle observations are enough to define shear strain and rotation of maximum shear.

- If both azimuth measurements and angle observations are performed, angular shear can be defined.

- By performing length measurements, dilatation and the parameters of symmetric strain tensor can be defined.

- The base line vectors that are derived from GPS measurements include scale and rotation information, all strain parameters can be determined.

4.5.1. Measurement or Adjusted Measurement Differences

Strain parameters can be obtained by comparing measurements or adjusted measurements in certain cases. This case is generally encountered in geodetic networks which do not have a convenient geometric structure. Correlations between raw measurements are not taken into account but when working with adjusted measurements correlations, the covariance matrix, is taken into account. Geodetic measurement differences can be denoted as functions of elements of strain tensor and rotation tensor by using Equation (4.5) in the form of coordinate differences (Demir,1999).

In a two dimensional coordinate system defined by x (north) and y (east) axes, below methods can be used;

- **Length measurement**

S_{ij} and S_{ij}' lengths are measured in t and t' periods in a direction which connects P_i and P_j points and has an αij angle with respect to x axis, variation of unit length ε_i is calculated by,

$$\varepsilon_i = \frac{\Delta S_{ij}}{S_{ij}.\Delta t} = \sin^2 \alpha_{ij}\ e_{xx} + \sin 2\,\alpha_{ij}\ e_{xy} + \cos^2 \alpha_{ij}\ e_{yy}$$

(4.22)

$$\Delta S_{ij} = S_{ij}{}' - S_{ij}\ ,\Delta t = \ t' - t$$

(4.23)

- **Azimuth**

α_{ij} and $\alpha_{ij}{}'$ are azimuth measurements from point P_i to point P_j in t and t' periods. The expression of their difference is denoted as in terms of tensor parameters.

$$\frac{\Delta \alpha_{ij}}{\Delta t} = \frac{1}{2}\sin 2\alpha_{ij}\ \left(e_{xx} - e_{yy}\right) + \cos 2\alpha_{ij} e_{xy} - \omega$$

(4.24)

- **Angle**

Angles measured on P_i point of a triangle which consists of P_i , P_j and P_k points are β_{jik} and $\beta_{jik}{}'$. The equation below shows the equation that can be used with their differences.

$$\frac{\Delta \beta_{jik}}{\Delta t} = \sin\beta_{jik}\left[\left(e_{xx} - e_{yy}\right)\cos\left(2\alpha_{ik} - \beta_{jik}\right) - 2e_{xy}\sin\left(2\alpha_{ik} - \beta_{jik}\right)\right]$$

(4.25)

4.5.2. Coordinate Differences

Coordinate differences, obtained by adjustment of surveys for each period of measurement or directly measured by space geodetic methods, are used in Equation (4.11).

$$u = e_{xx}x_i + e_{xy}y_i - \omega y_i + t_x$$

(4.26)

$$v = e_{xy}x_i + e_{yy}y_i + \omega y_i + t_y$$

In this model, strain tensor parameters are obtained by least squares estimation in which we take velocities that are obtained by processing of measurements in different periods.

4.5.3. Determination of Strain Parameters in an Adjustment Model

In this method strain parameters are obtained in the adjustment model together with other unknowns (coordinates *etc.*). Coordinates of point P_i in t' period is (x_i' , y_i'), and the functional model is,

$$x_i' = x_i + (t - t_0)[(\gamma_1/2 + \Delta)x_i + (\gamma_2/2 - \omega)y_i]$$

(4.27)

$$y_i' = y_i + (t - t_0)[(\gamma_2/2 + \omega)x_i + (\Delta - \gamma_1/2)y_i]$$

(Demir,1999)

In this model, the unknowns are, the x_i and y_i coordinates in t_0 time and strain parameters (γ_1, γ_2, ω, Δ). Coordinates and velocities in any time can be calculated by Equation (4.27).

4.5.4. Finite Differences Method

Assumption of homogenous strain field in all of the area which includes the deformation network is not realistic. This method is applied by dividing the area into sub areas with homogenous deformation characteristics. Different strain parameters area calculated for each sub area with the condition of sufficient points on each one of them. In this method sub areas are assumed to be triangles (Figure 4.5).
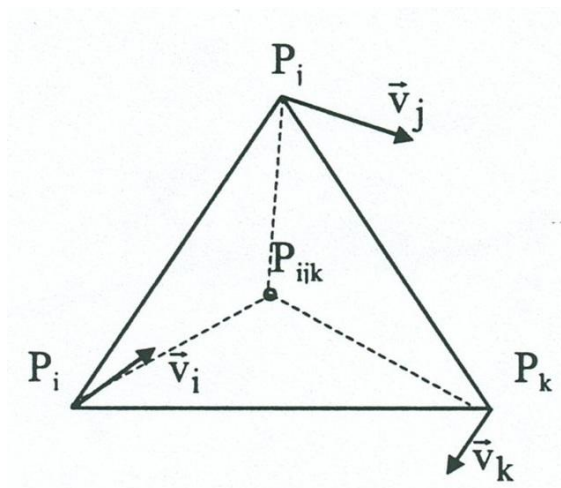
Figure 4.5. Finite differences method

Geodetic network is divided into triangles and by using the velocities on the corners of the triangle, strain parameters are calculated by (4.26) equations. If the variation of the length between the triangles corners is known, strain parameters can be directly calculated (Demir,1999).

4.5.5. Infinitesimal Homogenous Strain Model

This method relies on the assumption of that strain field varies from point to point but is homogenous on the point and its vicinity. Strain tensor parameters can be calculated if the length variation is known on point P in three directions. If length variation is known in more than three directions, least squares estimation is used. This calculation is performed for each point and strain tensor elements are calculated separately.
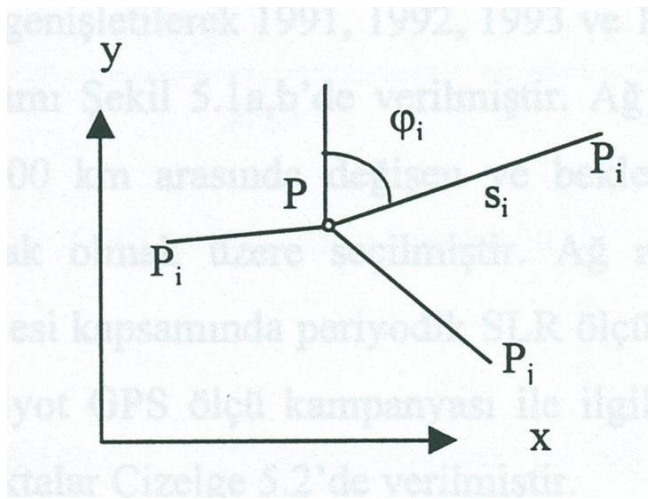
Figure 4.6. Infinitesimal homogenous strain model

4.5.6. Strain Results

Strain is calculated by using two different methods in this study. First method is finite differences method which is applied by using a script developed by Associate Prof. Dr. Bahadır Aktug in MATLAB environment. Geodetic network is divided into triangles and triangles' corners are the GPS campaign sites (Table 4.2). Triangles are chosen to be on and around the fault. All sites are not used in the triangulation process. Triangles are preferred to be equilateral and include the fault in their center. As these criteria are not

fulfilled by all the points in the study area, triangles are created by using the most suitable sites.

Table 4.2. Strain fields

Regions	Site Names
Triangle 1	GORC-ESEN-PTKV
Triangle 2	GORC-PTKV-TRAZ
Triangle 3	ESEN-URKM-PTKV
Triangle 4	URKM-ASKE-PTKV
Triangle 5	PTKV-TRAZ-ASKE
Triangle 6	TRAZ-ASKE-SFRH

There are 6 strain parameters to be calculated and two velocity components (north and east velocity) for each site are used in the calculations.
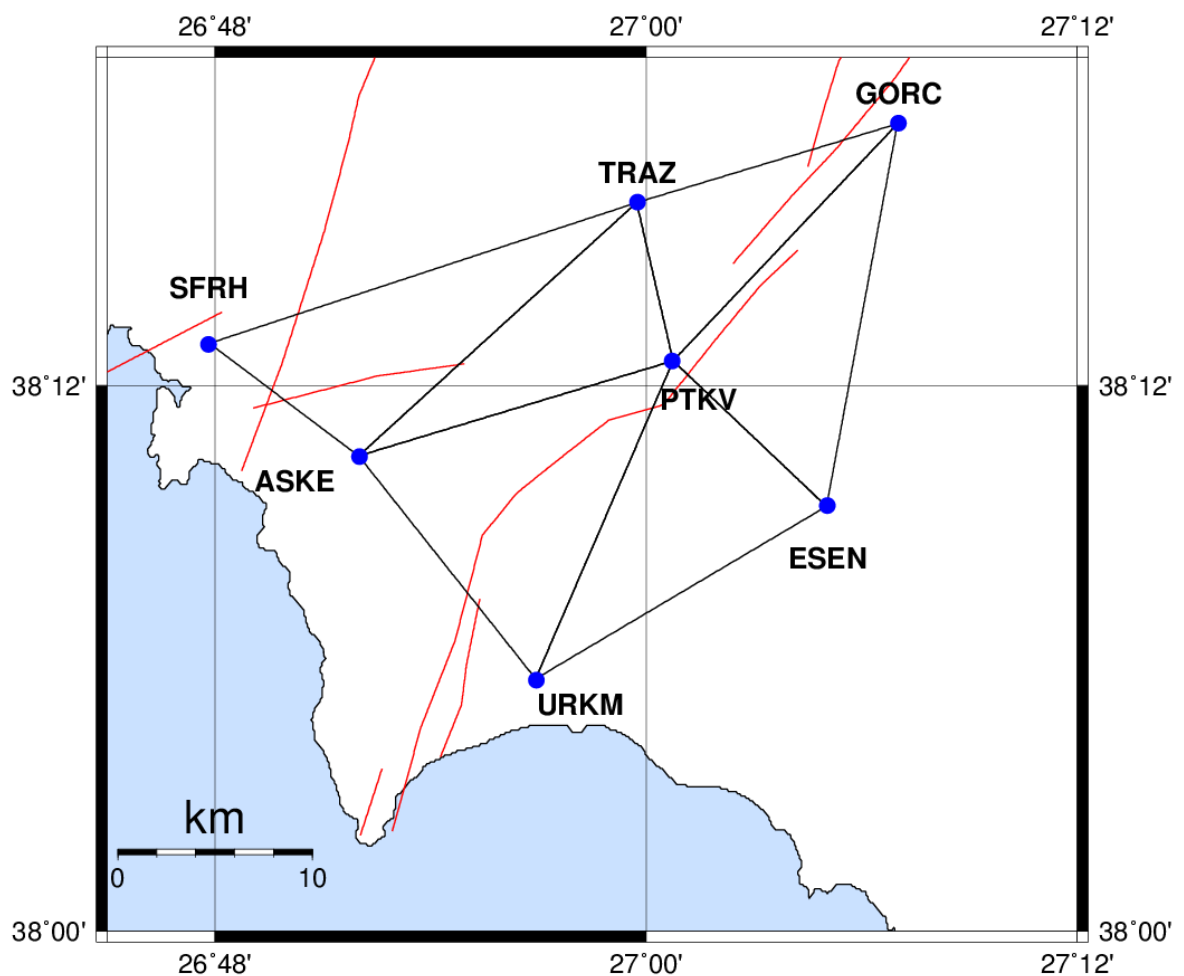
Figure 4.7. Triangles of the field

Strain is calculated on the baselines of each triangle and shown in the middle (Figure 4.8). It is assumed that strain is infinitesimal inside the triangle.
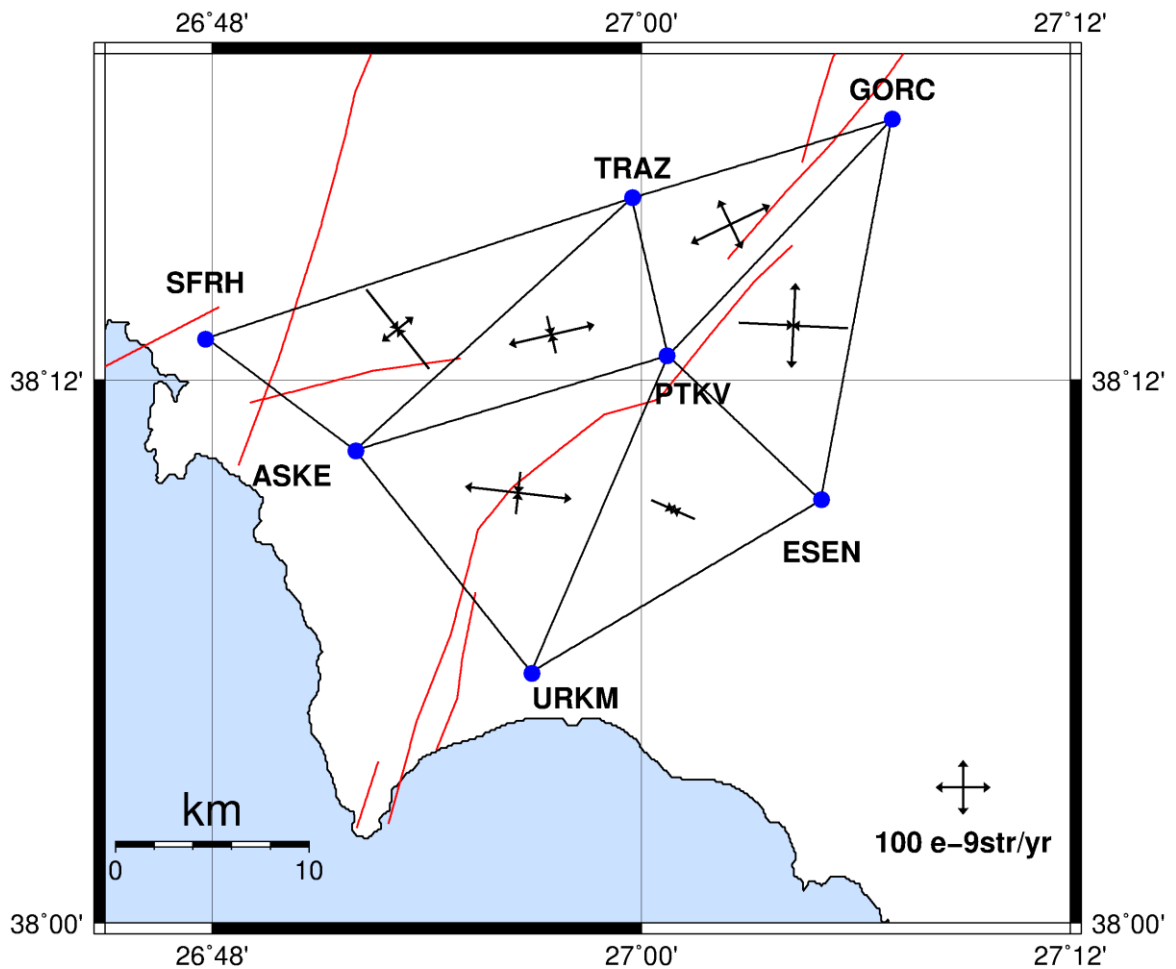
Figure 4.8. Results of finite differences method

After computation of strain tensor parameters, maximum and minimum principle strain components were calculated (Table 4.3).

Table 4.3 Calculated principal strains

Triangle	Latitude (deg)	Longitude (deg)	ε_1 $(10^{-9}/yr)$	ε_2 $(10^{-9}/yr)$	Azimuth (deg)
1	38.2201	27.0709	156.3878	-201.5034	272.7601
2	38.2572	27.0416	160.0642	97.7185	334.3257
3	38.1524	27.0149	18.9728	-87.1426	293.4834
4	38.1585	26.9426	196.3826	-77.4965	6.6481
5	38.2167	26.9582	160.1097	-68.9216	347.0351
6	38.2188	26.8865	73.2660	-185.6231	321.5866

The second algorithm was developed by Haines and Holt (1993) in order to estimate a strain rate and velocity model. This method was upgraded by Haines *et al.* (1998) and Beaven and Haines (2001), and applied in various regions (Holt and Haines 1995; Shen-Tu *et al.* 1999; Kreemer *et al.* 2000). A bicubic Bessel interpolation is used to expand a model rotation vector function which is obtained by a least-squares minimization, which is a best fit, between the model and the geodetic velocities. A comprehensive overview of the methodology can be found in Haines *et al.* (1998) (Doğru, 2008).

This algorithm uses the finite element method. FEM is an open solution in which a complex structure is broken into many small simpler components or finite elements. Each of the elements has nodes at each corner and at each midpoint. At these nodes, each element is attached to another. Within each separate element, a simple displacement field is assumed and the continuity of these fields enforced within the interpolation. Spline interpolation uses low-degree polynomials in each of the intervals, and chooses the polynomial pieces such that they fit smoothly together. The resulting function is called a spline. If the function has more than one variable, the method can be multivariate interpolation. This method includes bilinear interpolation and bicubic interpolation in two dimensions, and trilinear interpolation in three dimensions (Doğru, 2008).

One of the main advantages of this methodology is that an unlimited number of geodetic studies can be combined. The model velocity field provides a best fit to the observed vectors that have been rotated into a single model frame of reference (Kremer and Holt, 2000). For regions that are not densely sampled with geodetic observations, the interpolation of geodetic velocities can be highly non-unique in describing the regional strain rate field (Kreemer *et al.*, 2000b; Beavan and Haines, 2001).

According to Haines and Holt (1993), the horizontal velocity field u(r) for the spherical earth expressed as

$$u(\hat{x}) = rW(\hat{x}) \times \hat{x} \tag{4.28}$$

Where, r is the radius of the Earth and $\hat{x}$ is the position vector on the Earth's surface. This method allows the combination and comparison of different data types. It determines $W(\hat{x})$ at the nodes of a rectangular grid using bi-cubic spline interpolation. These values are obtained from least-squares inversion between observed and predicted values of strain rate and velocity. Depending on the data distribution on the study region, smoothing between neighboring grid cells is required. No smoothing takes no account of how the strain rates are distributed in neighboring rectangles, in which the strain rates may be significantly higher or lower. In the case of seismic data inversion, strain rates are estimated from Kostrov summation (1974);

$$\bar{\bar{\varepsilon}}_{ij} = \frac{1}{2\mu VT} \sum M_0 m_{ij} \tag{4.29}$$

Where, μ is the shear modulus, V is the cell volume (the grid area times the seismogenic thickness), T is the time period of the earthquake record, M_0 is the scalar seismic moment, and m_{ij} is the unit moment tensor. Shear modulus is taken as $3.5 \times 10^{10} Nm^{-2}$ and seismogenic thickness is 30 km. These chosen values affect the magnitude but not the style of the estimated strain rates.

Geodetic velocities are the changes in location of campaign-based GPS sites. These data are used as input data into a strain rate model which then calculated strain on an array over the study region. A spline interpolation technique is applied in which model velocities are fitted to observed GPS velocities, and those are then

interpolated to derive a continuous velocity gradient tensor field which implicitly defines the strain rate tensor everywhere. The model is calculated on a regular grid. Each grid area is 0.5° x 0.5° in dimension whether an area is considered to be deforming or not is based primarily on seismicity occurrence (Dogru A., 2010).

The obtained result of this algorithm is given in Table 4.4. Strain is calculated on the campaign sites in this method (Figure 4.9).
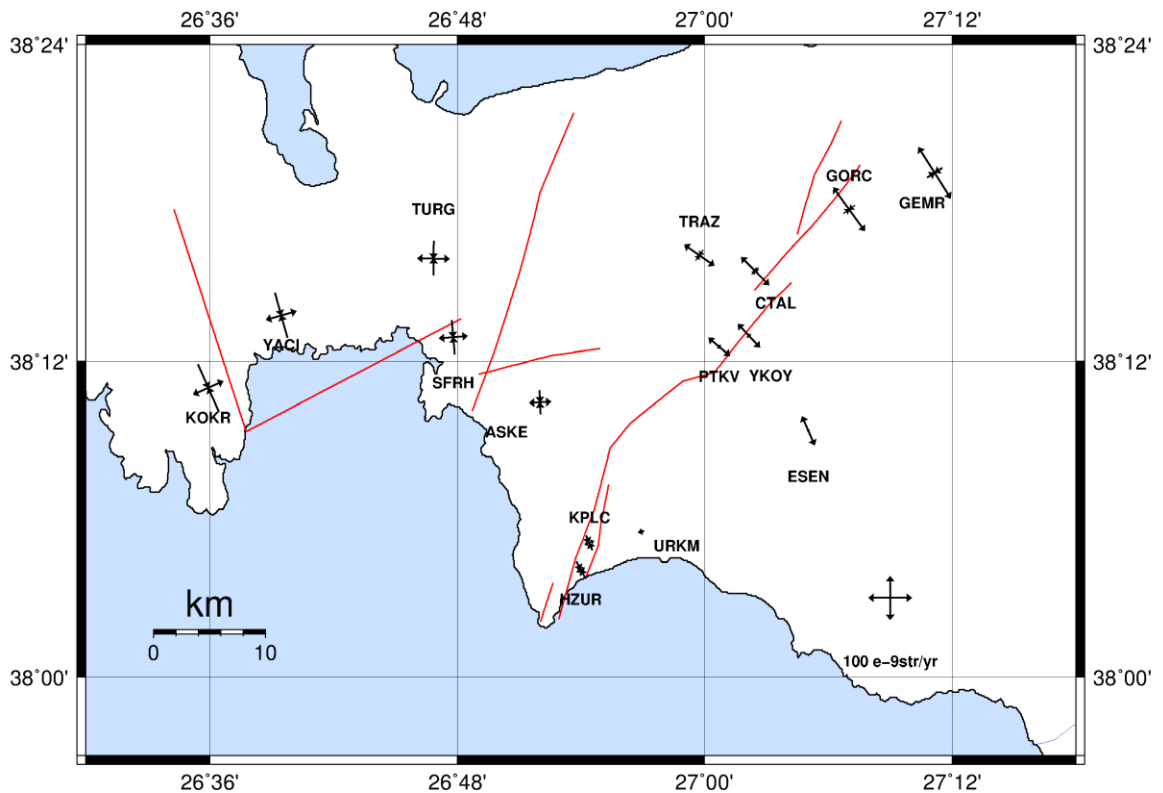
Figure 4.9. Results of Holt's algorithm

Table 4.4. Principal strains calculated by Holt's algorithm

Site	Latitude (deg)	Longitude (deg)	ε_1 (10^{-9}/yr)	ε_2 (10^{-9}/yr)	Azimuth (deg)
ESEN	38.15600	27.08400	-6.065538	73.349303	66.38791
CTAL	38.25700	27.04100	-21.328826	92.078124	45.33616
YKOY	38.21600	27.03600	-11.269108	74.666718	46.84353
PTKV	38.20900	27.01200	-11.241781	64.050750	39.62340
TRAZ	38.26700	26.99600	-29.591217	84.984958	34.76583
URKM	38.09200	26.94900	-14.412588	16.026610	161.21427
KPLC	38.08500	26.90700	-36.518712	23.571440	157.36406
HZUR	38.06800	26.90000	-41.540744	22.442156	151.75891
ASKE	38.17400	26.86700	-54.064907	50.311259	176.69603
SFRH	38.21500	26.79700	-78.222357	65.702838	175.13895
TURG	38.26500	26.78100	-79.412450	74.518305	1.04952
YACI	38.22900	26.65800	-105.91304	72.653598	164.14521
KOKR	38.18300	26.59900	-118.57978	75.603208	155.90785
GEMR	38.31900	27.18600	-40.814112	139.26156	57.62691
GORC	38.29600	27.11700	-32.379944	123.68109	53.97332

5. RESULTS AND DISCUSSION

Main purpose of this study is to calculate strain parameters by using the velocities of the sites which are established around the Tuzla Fault. The velocities of these sites are obtained by processing five GPS campaign data. GPS campaigns were carried out at 15 stations. Campaign dates were selected carefully to minimize the seasonal effects and same equipments were used at each site every year.

The obtained velocities vary between 25.08 mm/yr and 28.54 mm/yr with respect to Eurasia plate (Table 5.1). HZUR site has the greatest velocity and SFRH site has the smallest velocity.

Table 5.1. Velocity vector values

Site	Velocity (mm/yr)
GEMR	26.29 ∓ 1.95
GORC	25.87 ∓ 1.78
ESEN	25.10 ∓ 1.65
CTAL	26.96 ∓ 2.55
YKOY	27.89 ∓ 1.94
PTKV	27.50 ∓ 2.19
TRAZ	26.25 ∓ 2.03
URKM	27.77 ∓ 1.83
KPLC	27.94 ∓ 1.99
HZUR	28.54 ∓ 1.89
ASKE	26.27 ∓ 1.92
SFRH	25.08 ∓ 1.99
TURG	28.11 ∓ 1.97
YACI	26.62 ∓ 1.84
KOKR	28.08 ∓ 2.04

Aktug and Kilicoglu (2006) indicate that, velocity vectors in the area change between 20mm/yr to 30mm/yr (Figure 5.1). Velocity vectors are calculated with respect to Eurasia plate, in ITRF_2000 velocity field.
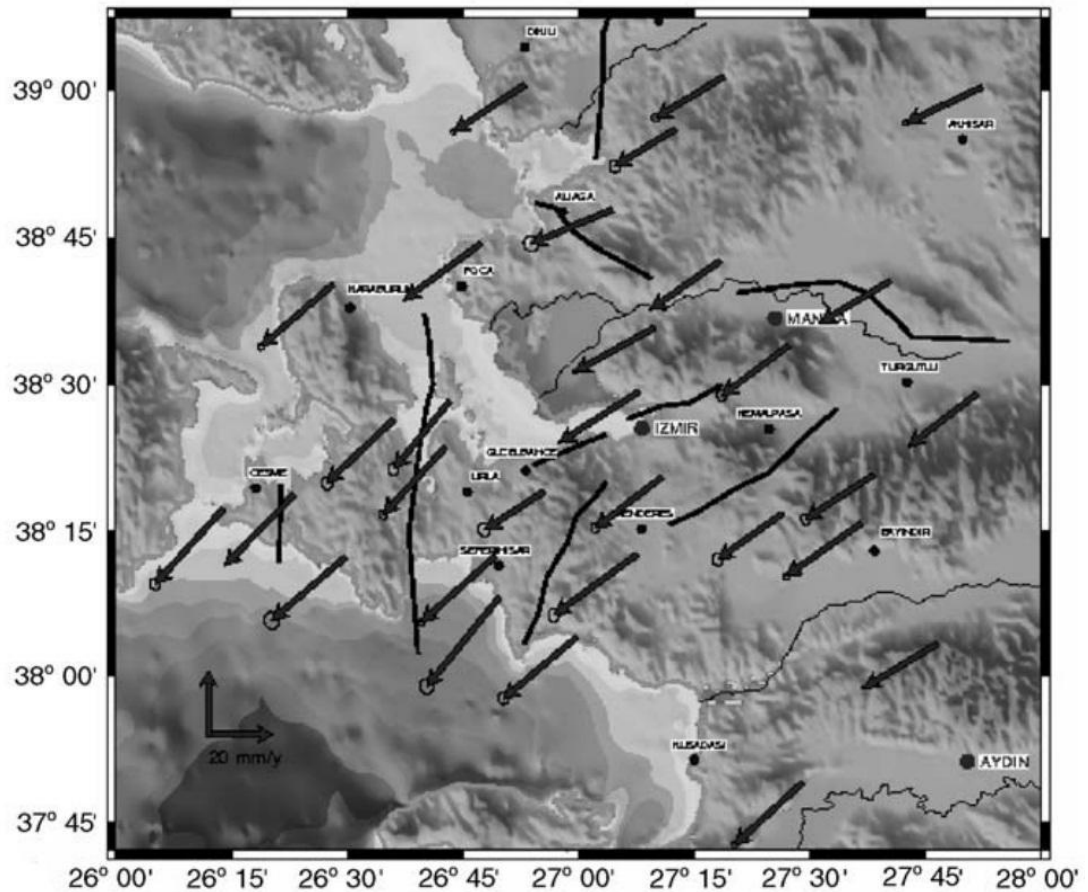
Figure 5.1. Velocities of Aktug and Kilicoglu (2006) with respect to Eurasia plate in ITRF_2000 velocity field

Aktug and Kilicoglu (2006) also gives the strain rates calculated by the velocities (Figure 5.2). Aktug and Kilicoglu (2006) include long term GPS observations from 1992 to 2004 and also cover a larger area. Table 5.2 gives the calculated maximum and minimum principal strain rates of this study which overlap with our study area.

Table 5.2. Strain rates of Aktug and Kilicoglu (2006)

Latitude (deg)	Longitude (deg)	ε_1 $(10^{-9}/yr)$	ε_2 $(10^{-9}/yr)$
37.95	26.87	100	-46
37.95	27.00	95	-30
37.95	27.13	82	-17
37.95	27.27	94	-18
38.08	26.60	183	-36
38.08	26.73	358	-29
38.08	26.87	483	-108
38.08	27.00	123	-96
38.08	27.13	89	-41
38.08	27.27	92	16
38.35	26.60	69	-44
38.35	26.73	116	-93
38.35	26.87	67	-176
38.35	27.00	57	-86
38.35	27.13	122	-19
38.35	27.27	83	58
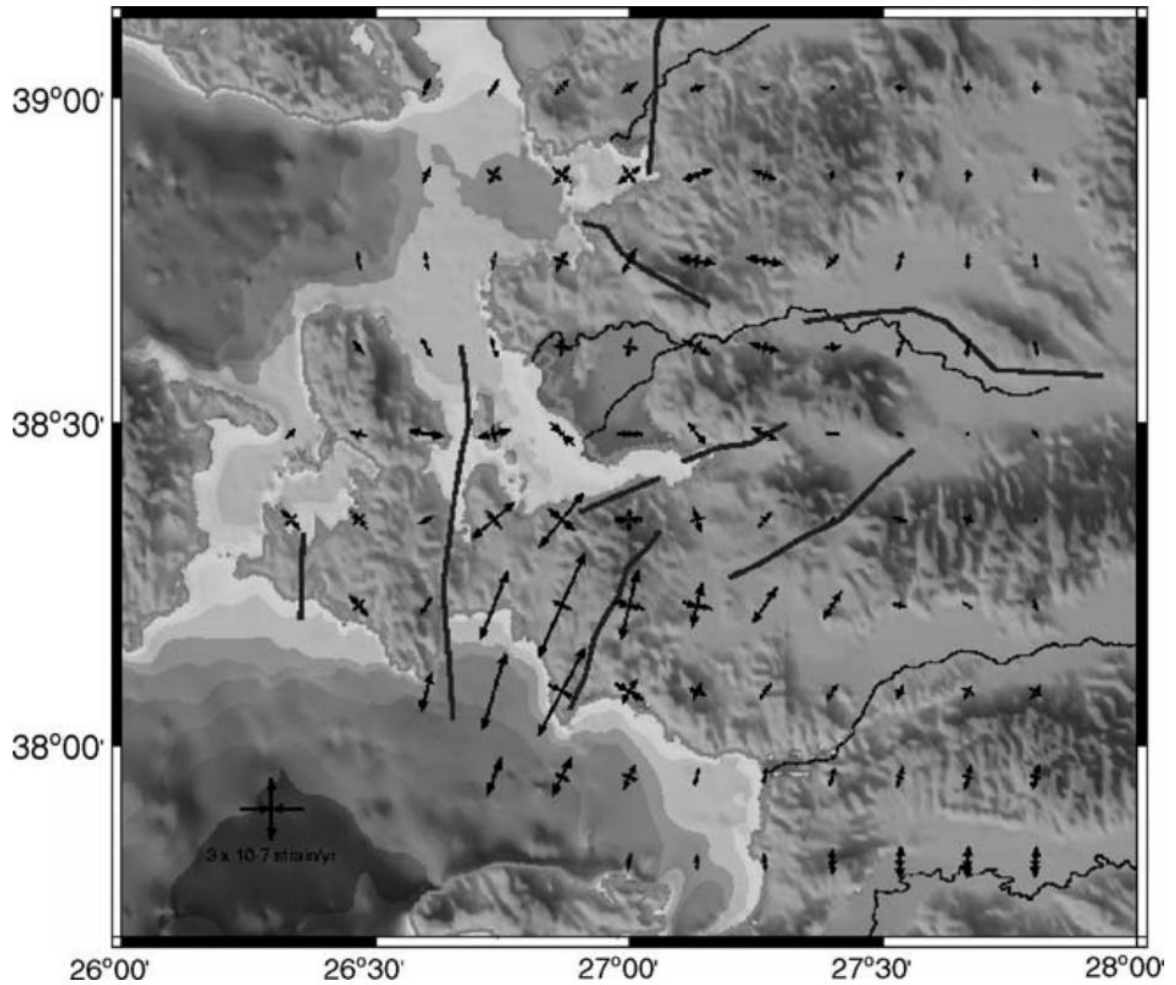
Figure 5.2. Strain rates of Aktug and Kilicoglu (2006)

In conclusion, the results of this study and prior studies indicate that, the Tuzla Fault is an active fault and has the potential to create a catastrophic earthquake which would affect millions of people. The characteristic NE-SW extension regime of the Aegean Region can be seen in the results. This study has been conducted by using the data of only five campaign measurements in three years. GPS measurements should be carried on to understand the kinematics of the Tuzla Fault.

REFERENCES

Aktug, B., and Kilicoglu A., 2006, "Recent Crustal Deformation of İzmir, Western Anatolia and Surrounding Regions as Deduced from Repeated GPS Measurements and Strain Field", *Journal of Geodynamics*, Vol. 41, No. 5, pp.471-484.

Altamimi, Z., P. Sillard, and C. Boucher, 2002, "ITRF2000: A New Release of the International Terrestrial Reference Frame for Earth Science Applications", *Journal of Geophysical Research*, 107 (B10), 2214, doi:10.1029/2001JB000561.

Altamimi, Z., X. Collilieux, J. Legrand, B. Garayt, and C. Boucher , 2007, "ITRF2005: A New Release of the International Terrestrial Reference Frame Based on Time Series of Station Positions and Earth Orientation Parameters", *Journal of Geophysical Research*, 112, B09401, doi:10.1029/2007JB004949.

Altunkaynak, Ş. ve Yılmaz, Y., 2000, "Foça Yöresinin Jeolojisi ve Aktif Tektoniği, Batı Anadolu." *Batı Anadolu'nun Depremselliği Sempozyumu (BADSEM 2000), Bildiriler Kitabı,* 160-165, İzmir.

Armijo, R., Meyer, B., King, G.C.P., Rigo, A., and Papanastassiou, D., 1996, "Quarternary Evolution of the Corinth Rift and its Implications for the Later Cenozoic Evolution of the Aegean" *Geophys. J. Int.,* 126, 11-53.

Arslan, A., 2007, *Analysis of Strain Accumulation of the Faulting Zones by the Help of Continuous GPS Stations*, M.Sc. Thesis, Boğaziçi University, KOERI, Istanbul.

Beavan, J., and Haines, J., 2001. "Contemporary Horizontal Velocity and Strain Rate Fields of the Pacific-Australian Plate Boundary Zone Through New Zealand", *Journal of Geophysical Research*, 106, 741-770.

Bradford W. Parkinson, James J. Spilker Jr. Eds., 1996, "GPS Error Analysis", *Global Positioning System: Theory and Applications* pages 478-483

Cakmak R., 2010, *Jeodezik Çalışmalarla Marmara Bölgesinde Deprem Döngüsünün Belirlenmesi ve Modellerle Açıklanması,* Ph.D. Dissertation, Istanbul Technical University, Geodesy and Photogrammetric Engineering, Istanbul.

Demir, C., 1999, *Kuzey Anadolu Fay Zonu Batı Kesiminde Yatay Yerkabuğu Hareketleri ve Gerinim Birikiminin Araştırılması*, Ph.D. Dissertaion, Yıldız Teknik Üniversitesi, İstanbul.

Doğru A., 2008, *Integration of Data Related to Earthquakes from a Variety of Disciplines in WEB-GIS,* PhD. Dissertation, Istanbul Technical University, Geodesy and Photogrammetric Engineering, Istanbul.

Doğru A., 2010, "Deformation of Eastern Turkey from Seismic and Geodetic Strain Rates", *Scientific Research and Essays*, Vol. 5 (9), pp. 911-916.

Emre, O., Barka, A., 2000, "Active Faults between Gediz Graben and Aegean Sea (İzmir Region)", *Proceedings of International Symposia on Seismicity of Western Anatolia*.

Emre, O., Ozalp, S., Dogaz, A., Ozaksoy, V., Yildirim, C., Goktas, F., 2005, *The Report on Faults of İzmir and its Vicinity and their Earthquake Potentials*, General Directorate of Mineral Research and Exploration Report No. 10754.

Erdogan, B., Altiner, D., Gungor, T., and Ozer, S., 1990, "Karaburun Yarım Adasının Stratigrafisi." *MTA Dergisi*, 111, 1-23.

Ergun, M., Oral, E. Z., 2000, "General Tectonic Elements of the Eastern Mediterranean and Implications" *Proceedings of International Symposia on Seismicity of Western Anatolia, İzmir*, 24-27 May.

Esder, T., Caglav, F., Pekatan, R., Yakabag, A., 1988, *Cumali-Tuzla (Seferihisar-İzmir) Jeotermal Sahasında Acılan Arama Kuyuları ve Sahanın Ön Fizibilite Raporu (in Turkish),* MTA Report No. 8146.

Floyd, A. M., 2008, *Continuous and Survey Global Positioning System Observation of the Deformation of the Aegean* , Ph.D. Dissertation, University of Oxford Department of Earth Sciences and Exeter College, Oxford.

Genc, C., Altunkaynak, S., Karacik, Z., Yazman, M., Yilmaz, Y., 2001, "The Cubuklu Graben, South of İzmir: Tectonic Significance in the Neogene Geological Evolution of the Western Anatolia.", *Geodinamica Acta*, Vol. 14, No. 1/3, pp. 45-55.

Haines, A.J. and Holt, W.E., 1993. "A Procedure to Obtain the Complete Horizontal Motions Within Zones of Distributed Deformation From the Inversion of Strain Rate Data", *Journal of Geophysical Research*, 98, 12,057-12,082.

Haines, A.J., Jackson, J.A., Holt, W.E., Agnew, D.C., 1998, "Representing Distributed Deformation by Continuous Velocity Fields", *Institute of Geological and Nuclear Sciences science report,* 98/5, Wellington, New Zealand.

Halıcıoğlu, K., Özener, H., 2008, "Geodetic Network Design and Optimization on the Active Tuzla Fault (İzmir, Turkey) for Disaster Management", *Sensors*, 8, pp. 4741-4757.

Herring, T. A., King, R. W., McClusky, S. C., 2010a, "GAMIT Reference Manual GPS Analysis at MIT Release 10.3" *Department of Earth, Atmospheric, and Planetary Sciences* Massachussetts Institute of Technology,.

Herring, T. A., King, R. W., McClusky, S. C., 2010b, "Introduction to GAMIT/GLOBK Release 10.3", *Department of Earth, Atmospheric, and Planetary Sciences* Massachusetts Institute of Technology.

Herring, T. A., King, R. W., McClusky, S. C., 2010c, "Global Kalman Filter VLBI and GPS Analysis Program" *Department of Earth, Atmospheric, and Planetary Sciences* Massachusetts Institute of Technology.

Holt, W.E. and Haines, A.J., 1995, "The Kinematics of Northern South Island New Zealand Determined From Geologic Strain Rates", *Journal of Geophysical Research*, 100, 17991-18010.

Divener, V., 2006, Stress and Strain - Rock Deformation, Long Island University Course Notes, http://myweb.cwpost.liu.edu/vdivener/notes/stress-strain.htm

Nelson, S. A., 2003, Deformation of Rock, Tulane University Physical Geology Course Notes, http://www.tulane.edu/~sanelson/geol111/deform.htm

İDSDMP: İzmir Deprem Senaryosu ve Deprem Master Planı, http://www.izmirbld.gov.tr/izmirdeprem/izmirrapor.htm

Jackson, J., and D. McKenzie, 1988, "The Relationship Between Plate Motions and Seismic Moment Tensors and the Rates of Active Deformation in the Mediterranean and Middle East", *Geophys. J. R. Astr. Soc.*, 93 (1), 4573, doi:10.1111/j.1365-246X.1988.tb01387.x.

Jackson, J., Haines, J. & Holt, W., 1994, "A Comparison of Satellite Laser Ranging and Seismicity Data in the Aegean Region", *Geophysical Research Letters*, Vol. 21, pp. 2849-2852.

Jaeger, J.C., 1969, "Elasticity, Fracture and Flow", *Methuen, London*, pp:268.

Kahveci M., 2009, *GPS : Teori ve Uygulama*, Nobel Yayın Dağıtım, İstanbul.

Kocyigit, A., 2000, "Seismicity of Southwestern Turkey", *Proceedings of International Symposia on Seismicity of Western Anatolia,* İzmir.

Kreemer, C., Holt, W.E., Goes, S., Govers, R., 2000, "Active Deformation in Eastern Indonesia and the Philippines From GPS and Seismicity Data", *Journal of Geophysical Research*, 105, 663-680.

Mase, G.E., 1970, "Continuum Mechanics, Schaum's Outline Series", *Mc Graw-Hill Company*, Newyork.

Mc Clusky, S., Balassanian, S., Barka, A., Demir, C., Ergintav, S., Georgiev I., Gurkan, O., Hamburger, M., Hurst, K., Kahle, H., kastens, K., Kekelidze, G., King, B., Kotzev, V., Lenk, O., Mahmoud, S., Mishin, A., Nadaria, M., Ouzoun,s, A., Paradissis, D., Peter, Y., Prilepin, M., Reilinger, R., Sanli, I., Seeger, H., Tealeb, A., Toksoz, M. N., Veis, G., 2000, "Global Positioning System Constraints On Plate Kinematics And Dynamics In The Eastern Mediterranean And Caucasus", *Journal of Geophysical Research*, Vol. 105, No. B3, pp. 5695-5719.

Mc Kenzie, D. P., 1972, "Active Tectonics of the Mediterranean Region", *Geophysical Journal of Research*, Vol. 30, pp.109-185,

Mc Kenzie, D., 1978, "Active Tectonics of Alphine-Himalayan Belt: The Aegean Region and Surrounding Regions", *Geophysical J. R. Ast. Soc.*, Vol. 55, pp. 217-254,

Mercier, J., Sorel, D., Vergely, P., Simeakis, K., 1989, "Extensional Tectonic Regimes in the Aegean Basins during the Cenozoic", *Basin Research*, Vol. 2, pp. 49-71

Mierlo, J., 1981, "Some Aspect of Strain Analysis by Geodetic Methods", *Forty Years of Thought*, Vol II, pp:507-526.

Monroe J. S., 1996, *Physical Geology*, Thomson Learning.

Müller, S., Kahle, H. G., and Barka, A., 1997, "Plate Tectonics Situation in the Anatolian-Aegean Region", *Active Tectonics of Northwestern Anatolia- the Marmara Poly-project*.

Ocakoglu, N., Demirbas, E., Kuscu, I., 2005, "The Submarine Active Faults and the Seismicity of the Gulf of İzmir and Surrounding Area" *Journal of the Earth Sciences Application and Research Centre of Hacettepe University*, Vol. 27(1), pp. 23-40, b.

Ozener H., 2010, "The Importance of Tuzla Fault and a Study on Deformation Monitoring in the Aegean Region, Turkey", *FIG Congress*, Sydney, Australia.

Ozener H., Dogru A., Acar M., 2012, "Determination of the displacements along the Tuzla fault (Aegean region-Turkey): Preliminary results from GPS and precise leveling techniques", *Journal of Geodynamics*,http://dx.doi.org/10.1016/j.jog.2012.06.001

Papazachos, C. B., 1999, "Seismological and GPS Evidence for the Aegean Anatolia Interaction", *Geophysical Research Letters*, Vol. 17, pp. 2653-2656.

Piper, J., Gursoy, H., and Tatar, O., 2001, "Paleomagnetic Analysis of Neotectonic Crustal Deformation in Turkey", *Proceeding of Symposia on Seismotectonics of the North-Western Anatolia-Aegean and Recent Turkish Earthquakes*.

Prescott, W, H., Savage, J.C., and Kinoshita, W. T., 1979, "Strain Accumulation Rates in the Western United States Between 1970 and 1978", *Journal of Geophysical Research*, Vol.84, No. B10, 5423-5435.

Reilinger, R., McClusky, S., Vernant, P., Lawrence,S., Ergintav, S., Cakmak, R., Ozener, H., Kadirov, F., Guliev, I., Stepanyan, R., Nadariya, M., Hahubia, G., Mahmoud, S., Sakr, K., ArRajehi, A., Paradissis, D., Al-Aydrus, A. Prilepin, M., Guseva, T., Evren, E., Dmitrotsa, A., Filikov, S. V., Gomez, F., Al-Ghazzi, R., Karam, G., 2006, "GPS Constraints on Continental Deformation in the Africa-Arabia-Eurasia Continental Collision Zone and implications for the Dynamics of Plate Interactions", *Journal of Geophysical Research*, Vol.111, B05411.

Sabuncu, A., Ozener, H., 2010, "Determination of the Displacements along the Tuzla Fault (İzmir) and Surroundings by GPS and Precise Leveling Techniques", *WEGENER 2010-15th General Assembly of WEGENER*, Istanbul-Türkiye.

Saroglu, F., Emre, O. and Boray, A. 1987, "Türkiye'nin Diri Fayları ve Depremselliği". *MTA, Rapor No: 8174.*

Saroglu, F., Emre, Ö., ve Kuşçu, İ., 1992, *Türkiye Diri Fay Haritası, 1:2,000,000 ölçekli*, Maden Tetkik ve Arama Genel Müdürlüğü, Ankara.

Shen-Tu, B., W. E. Holt, A. J. Haines, 1999, "The Kinematics of the Western United States Estimated From Quaternary Rates of Slip and Spacegeodetic Data", *Journal of Geophysical Research*, 104, 28927-28955.

Sodoudi, F., 2005, "*Lithospheric Structure of the Aegean Obtained from P and S receiver Functions*", Ph.D. Dissertation, TU Berlin.

Straub, C., Kahle, H. G., Schindler, C., 1997, "GPS and Geological Estimates of the Tectonic Activity in the Marmara Sea Region, NW Anatolia", *Journal of Geophysical Research*, 102, B12, 27587-27601.

Tan, O. ve Taymaz, T., 2001, "Source parameters of November 6, 1992 Doğanbey (İzmir) Earthquake (Mw=6.0) Obtained From Inversion of Teleseismic Body-Waveforms". *4th International Turkish Geology Symposium, 24–28 September 2001*, Çukurova University, Abstract volume, p. 171, Adana.

Taymaz, T., 2001, "Active Tectonics of the North and Central Aegean Sea" *Proceeding of Symposia on Seismotectonics of the North-Western Anatolia-Aegean and Recent Turkish Earthquakes*.

UNAVCO Campaign GPS_GNSS Handbook

Utku, M., 2000, "Position of Western Anatolia in Turkey's Seismicity", *Proceedings of International Symposia on Seismicity of Western Anatolia*.

Vanicek, P., Thapa, K., and Schneider, D., 1981, "The Use of Strain to Identify Incompatible Observations and Constraints in Horizontal Geodetic Networks", *Manuscripta Geodaetica*, Vol.6, pp:257-281.

Welsch, W., 1981, "Description of Homogeneous Horizontal Strains and Some Remarks", *IAG Sym. On Geodetic Networks and Computaion*, DGK, Reihe B, H. 258/V, pp:188-205.

Wessel, P. and W. H. F. Smith, 1991, "Free Software Helps Map and Display Data", *EOS Trans.* AGU, 72, 441.

Yildiz F., Kahveci M., 2009, "*GPS/GNSS Uydularla Konum Belirleme Sistemleri*", Nobel Yayin Dagitim / Teknik Bilimler Dizisi, Aralik.

Yilmaz, Y., 2000, "Active Tectonics of Aegean Region", *Proceedings of International Symposia on Seismicity of Western Anatolia*, İzmir.

APPENDIX

ASKE North Offset   4249529.371 m
rate(mm/yr)= −15.29 ± 1.43 nrms= 0.70 wrms=   2.2 mm # 5
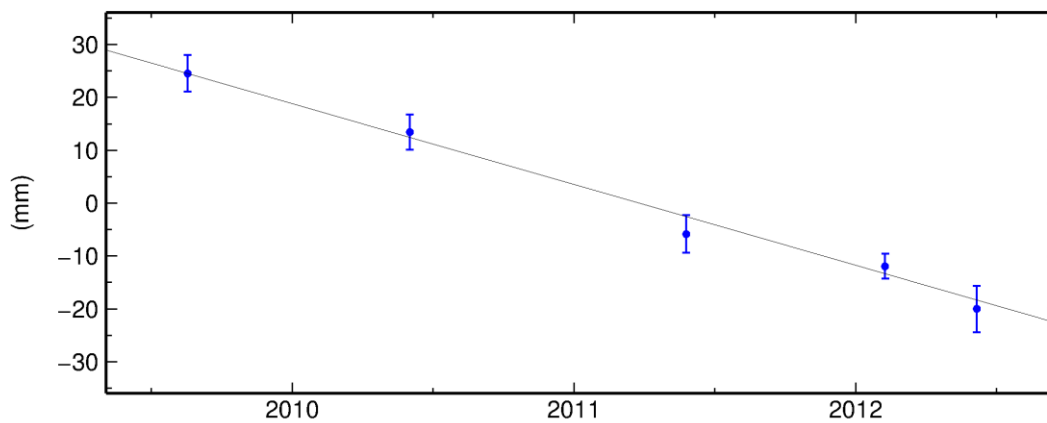
ASKE East Offset   2351192.880 m
rate(mm/yr)= −19.21 ± 1.30 nrms= 1.12 wrms=   3.3 mm # 5
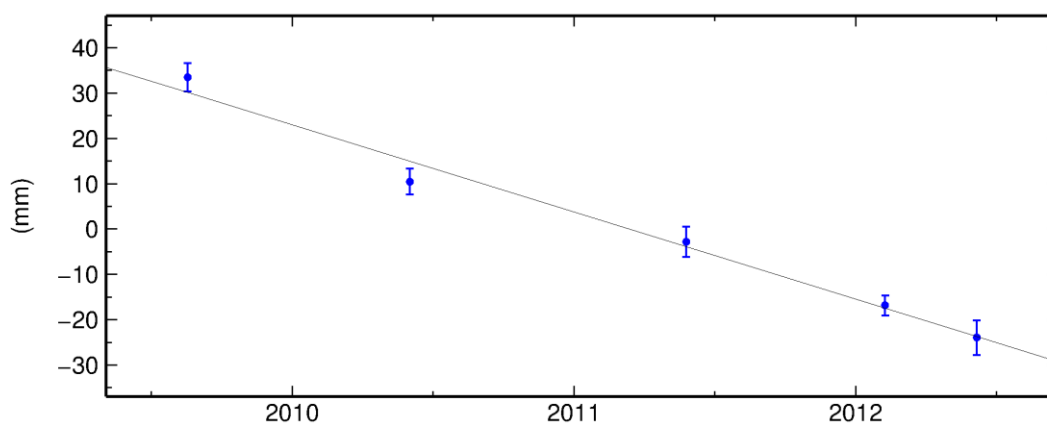
ASKE Up Offset   120.673 m
rate(mm/yr)= −0.35 ± 5.67 nrms= 0.73 wrms=   9.5 mm # 5

GMT 2012 Jul 09 17:22:35   p: 1
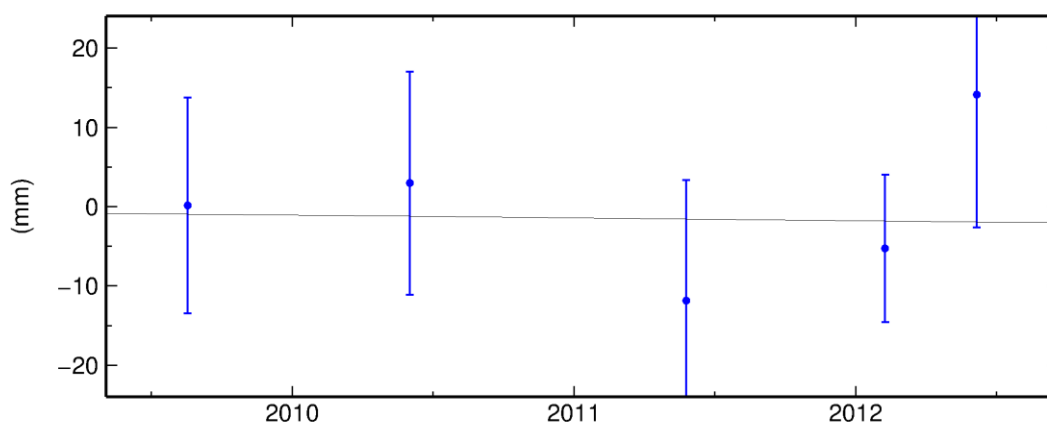
CTAL North Offset   4258761.322 m
rate(mm/yr)= −16.13 ± 1.90 nrms= 1.12 wrms=   5.3 mm # 5
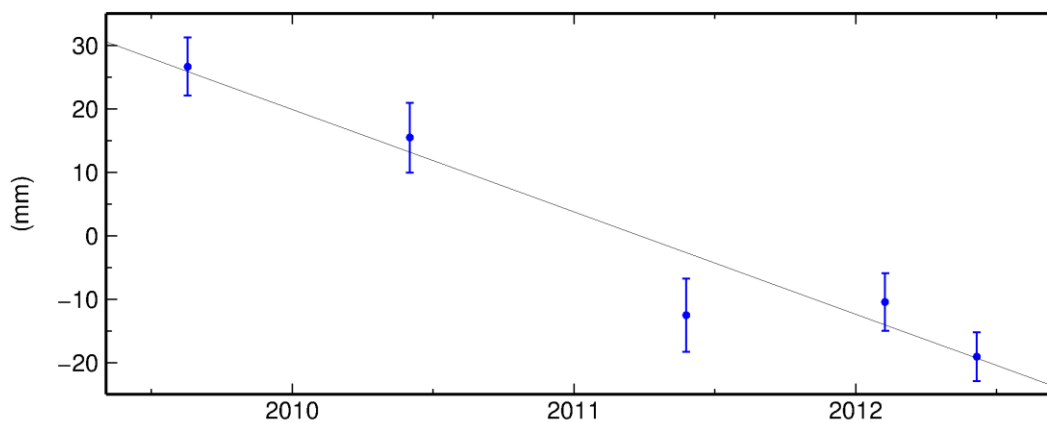
CTAL East Offset   2363785.463 m
rate(mm/yr)= −20.15 ± 1.71 nrms= 0.44 wrms=   1.9 mm # 5
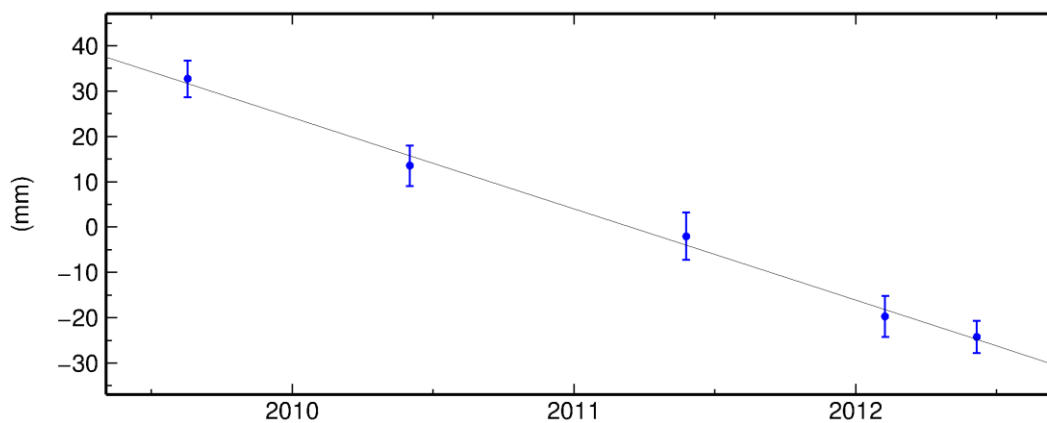
CTAL Up Offset   381.997 m
rate(mm/yr)= 305.30 ± 7.87 nrms= 25.01 wrms= 497.6 mm # 5
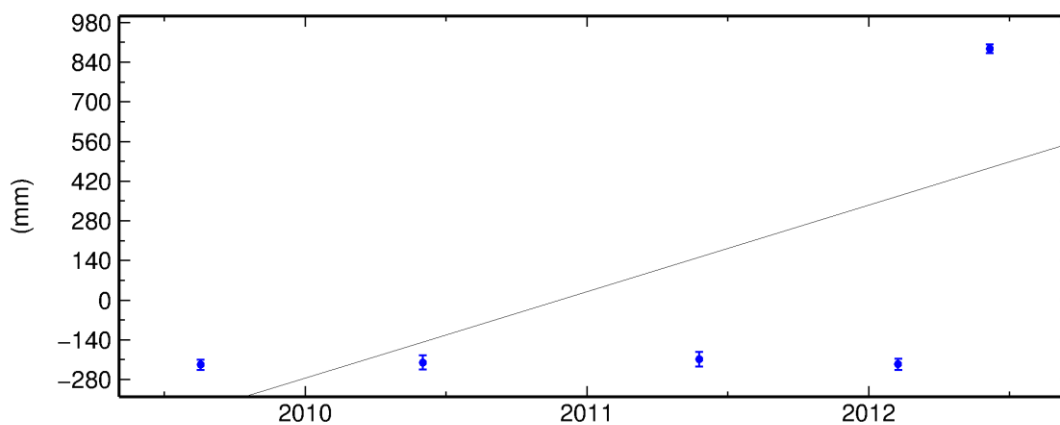
ESEN North Offset   4247470.230 m
rate(mm/yr)= −13.43 ± 1.21 nrms= 0.76 wrms= 2.0 mm # 5
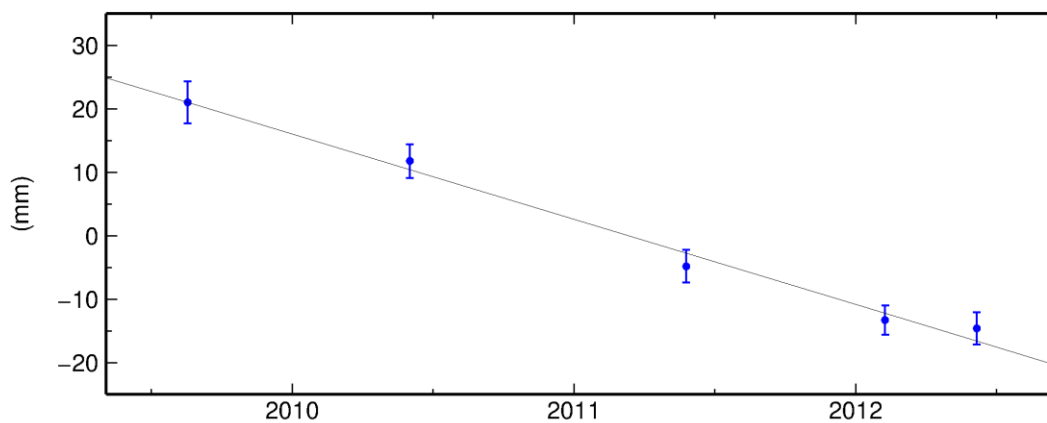
ESEN East Offset   2370744.416 m
rate(mm/yr)= −18.75 ± 1.12 nrms= 0.68 wrms= 1.7 mm # 5
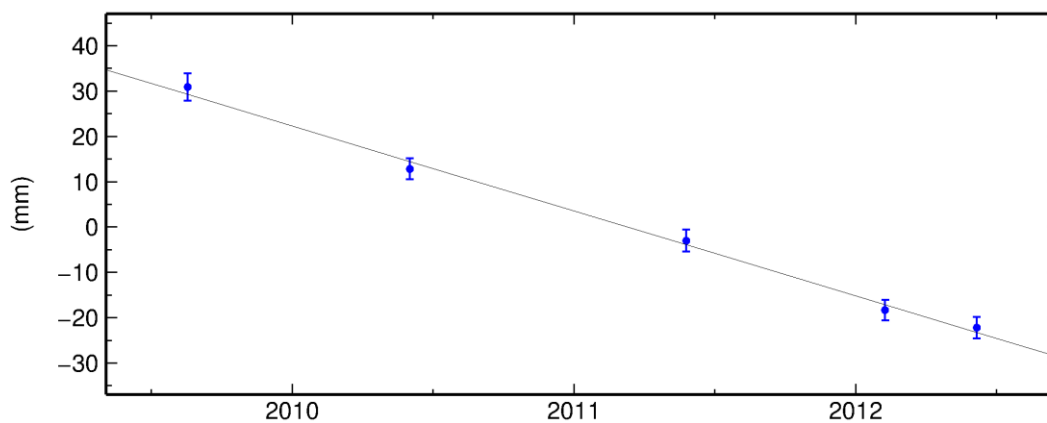
ESEN Up Offset   139.939 m
rate(mm/yr)=   2.75 ± 4.91 nrms= 0.42 wrms= 4.5 mm # 5

GMT 2012 Jul 09 17:22:37   p: 4
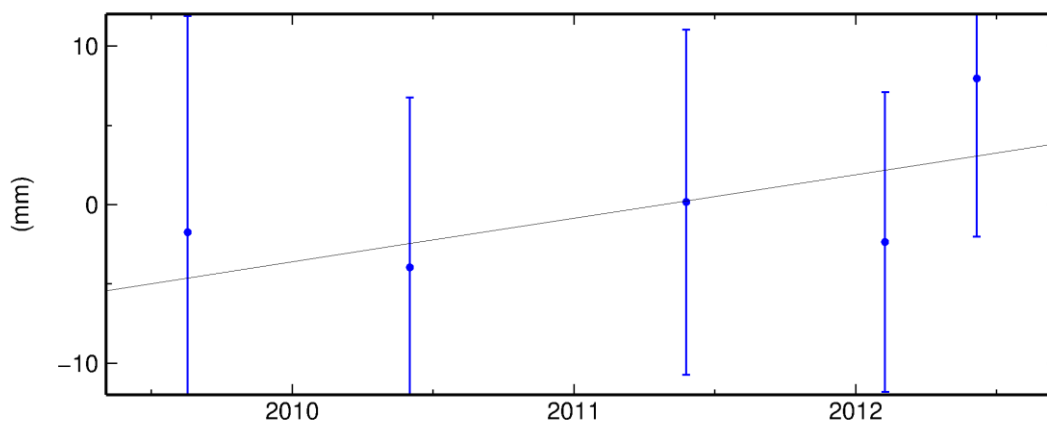
GEMR North Offset   4265644.249 m
rate(mm/yr)= −14.44 $\pm$ 1.45 nrms= 0.69 wrms=   2.2 mm # 5
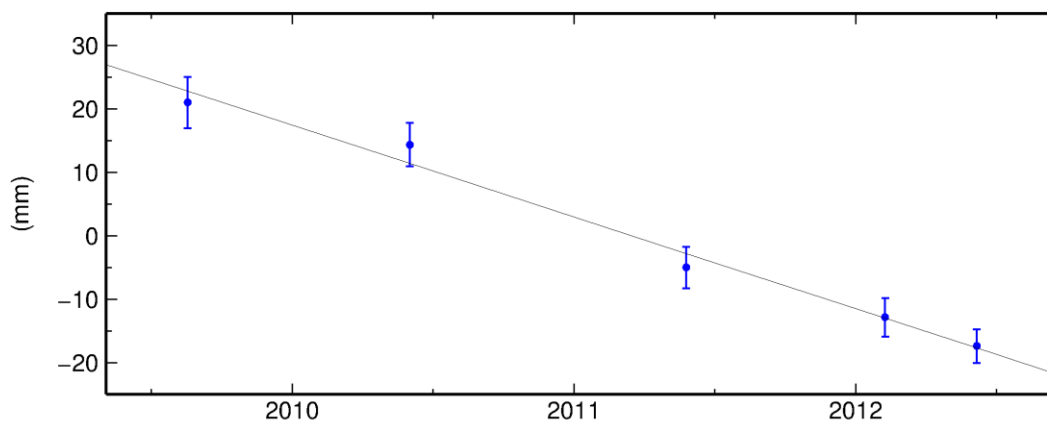
GEMR East Offset   2374354.867 m
rate(mm/yr)= −19.54 $\pm$ 1.31 nrms= 1.04 wrms=   3.1 mm # 5
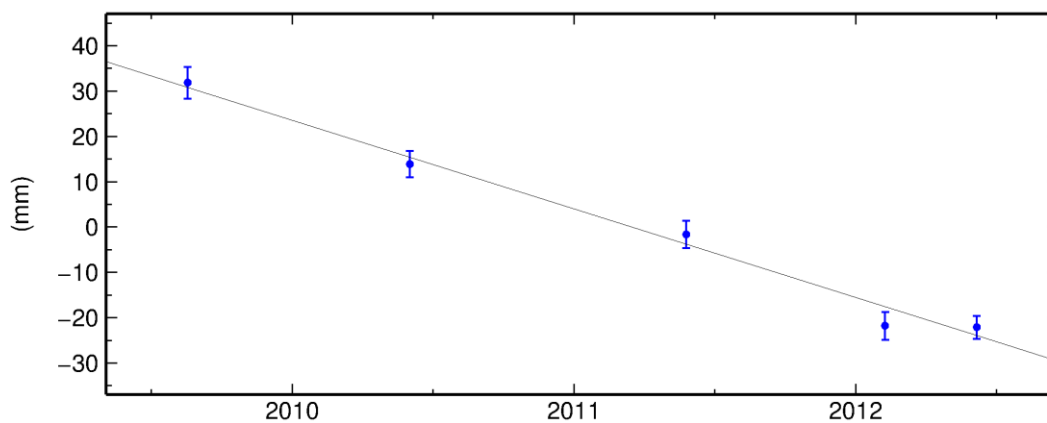
GEMR Up Offset   217.578 m
rate(mm/yr)= −25.57 $\pm$ 5.78 nrms= 2.86 wrms= 36.9 mm # 5

GMD 2012 Jul 09 17:22:38   p: 5
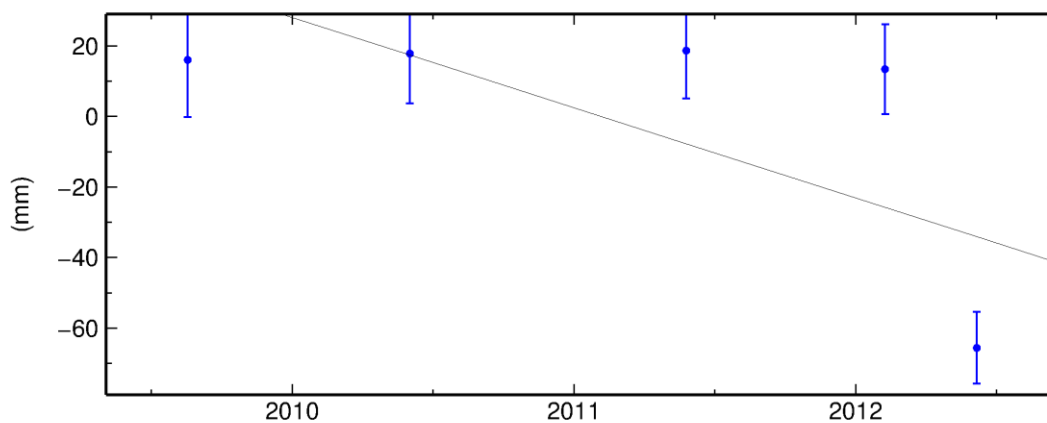
GORC North Offset   4263059.564 m
rate(mm/yr)= −15.86 ± 1.32 nrms= 0.65 wrms= 2.1 mm # 5
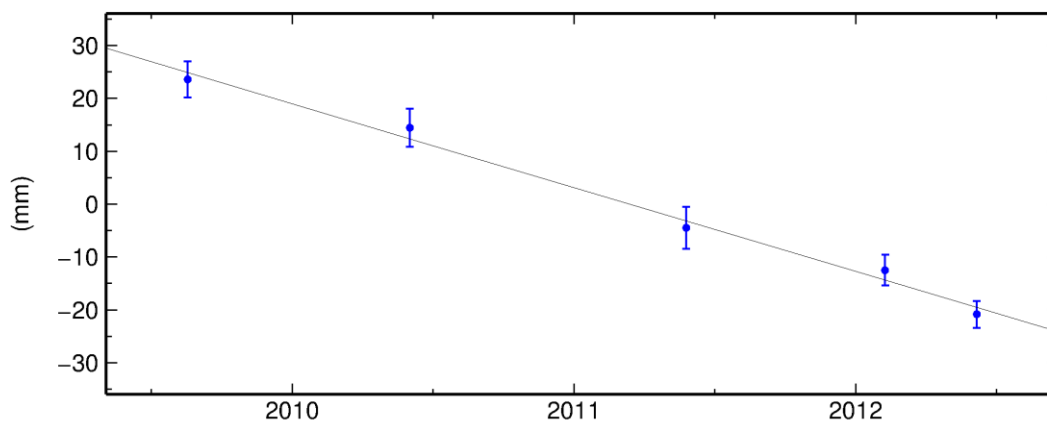
GORC East Offset   2369051.450 m
rate(mm/yr)= −17.79 ± 1.20 nrms= 0.86 wrms= 2.5 mm # 5
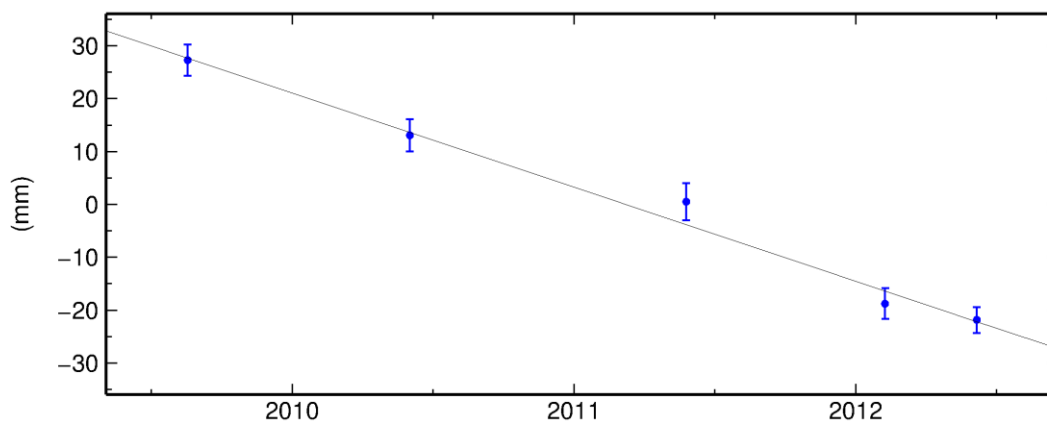
GORC Up Offset   269.654 m
rate(mm/yr)= 30.10 ± 5.20 nrms= 3.37 wrms= 42.5 mm # 5

2012 Jul 09 17:22:39   p: 6
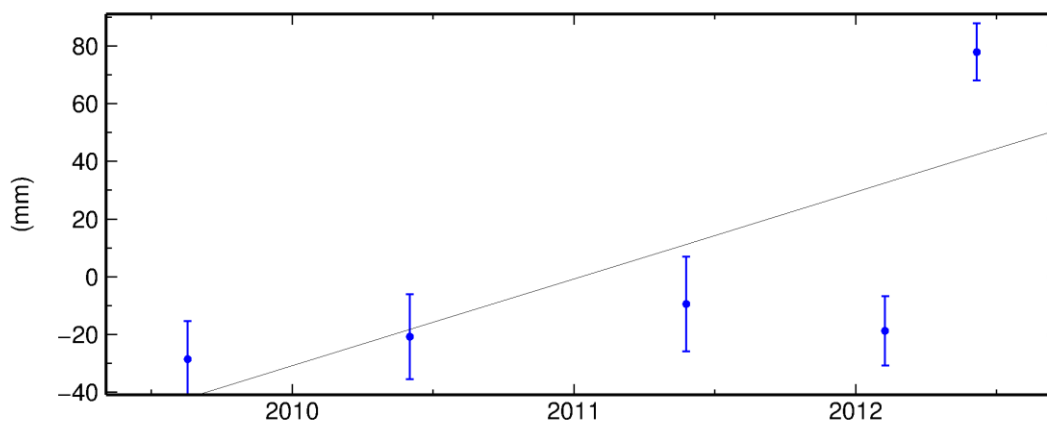
HZUR North Offset   4237675.824 m
rate(mm/yr)= −19.34 ± 1.41 nrms= 0.72 wrms= 2.1 mm # 4
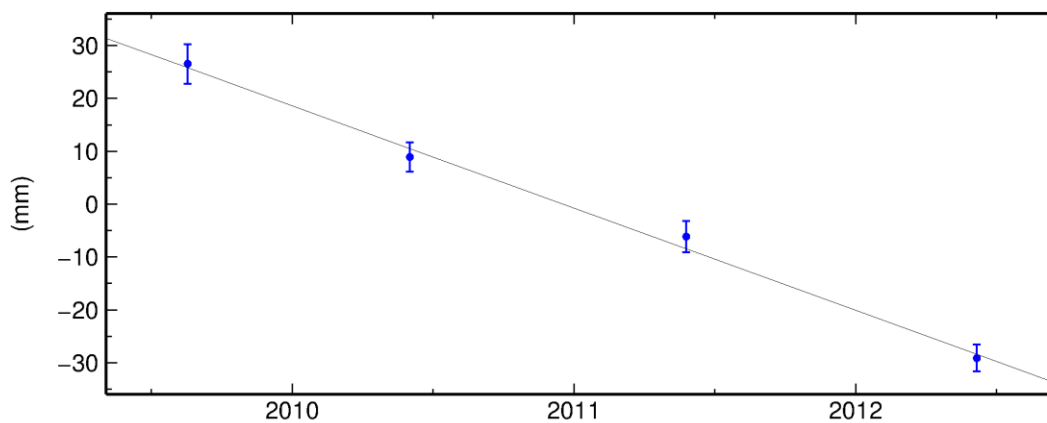
HZUR East Offset   2357569.430 m
rate(mm/yr)= −17.86 ± 1.31 nrms= 0.75 wrms= 2.0 mm # 4
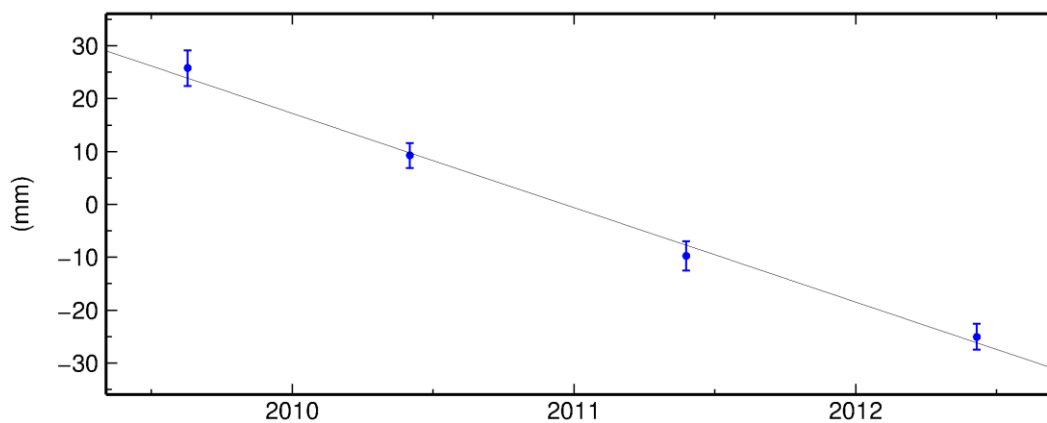
HZUR Up Offset   56.193 m
rate(mm/yr)= −60.52 ± 5.56 nrms= 8.84 wrms= 103.1 mm # 4

GMD 2012 Jul 09 17:22:40   p: 8
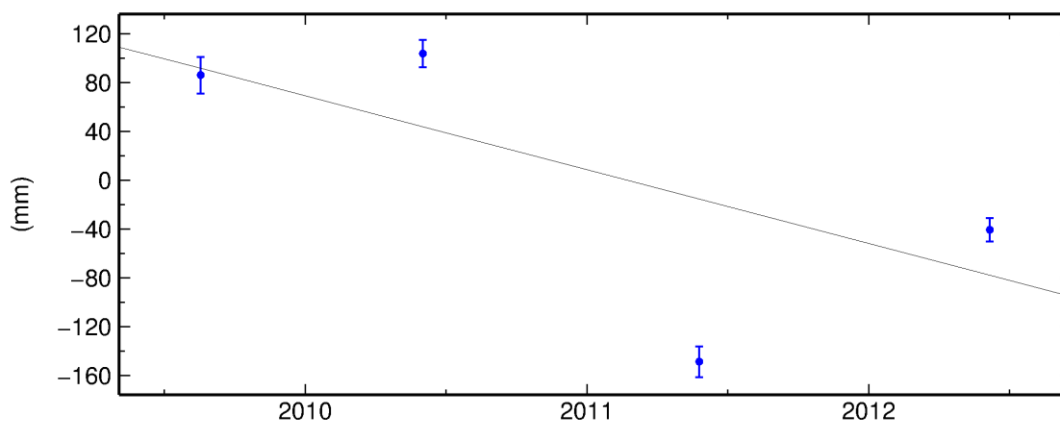
KOKR North Offset   4250501.621 m
rate(mm/yr)= −18.78 ± 1.51 nrms= 0.81 wrms= 2.7 mm # 5
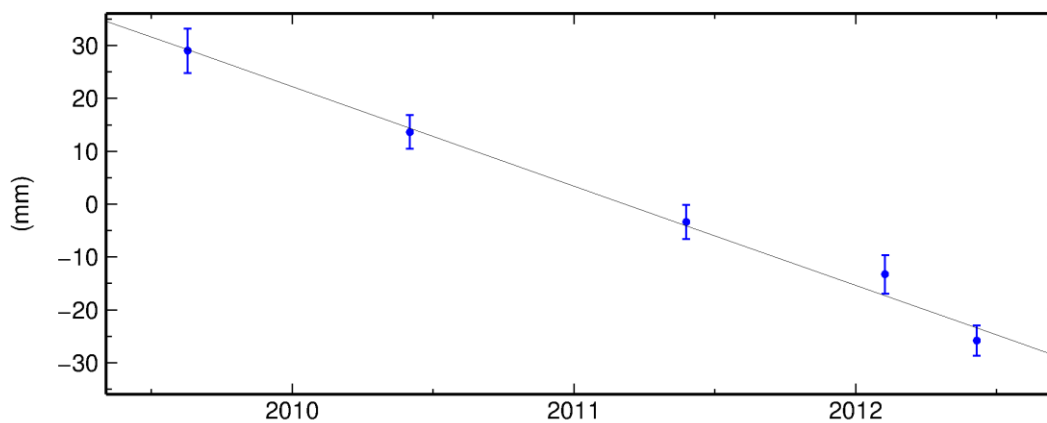
KOKR East Offset   2327529.310 m
rate(mm/yr)= −17.70 ± 1.39 nrms= 1.19 wrms= 3.7 mm # 5
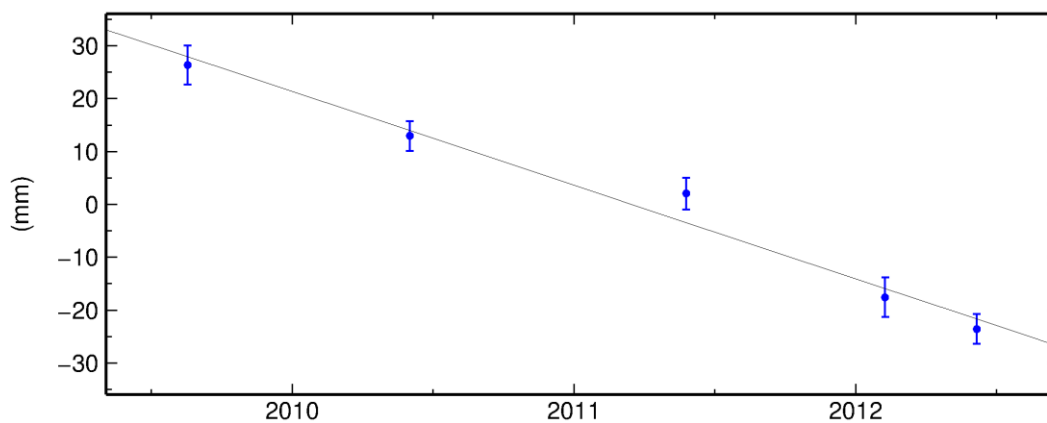
KOKR Up Offset   370.780 m
rate(mm/yr)= −8.31 ± 6.15 nrms= 0.96 wrms= 13.3 mm # 5

GMD 2012 Jul 09 17:22:42   p: 11
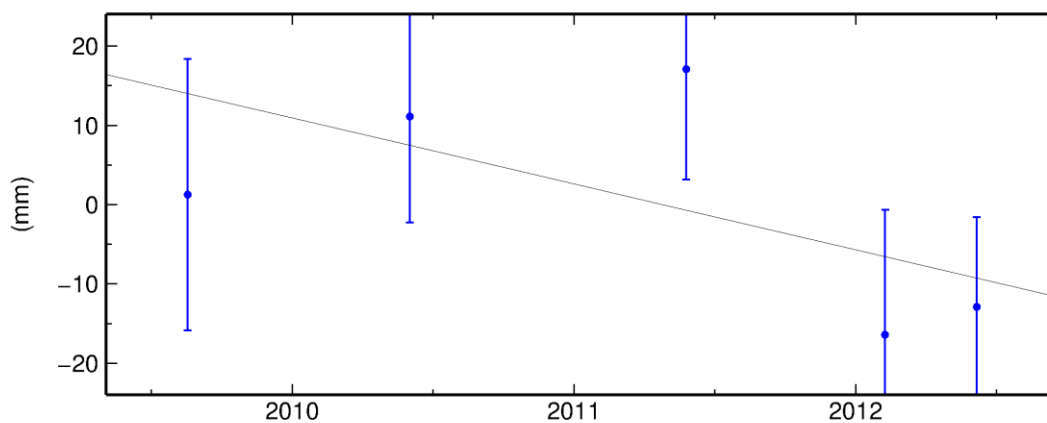
KPLC North Offset   4239621.571 m
rate(mm/yr)= −18.97 ± 1.51 nrms= 0.79 wrms= 2.6 mm # 5
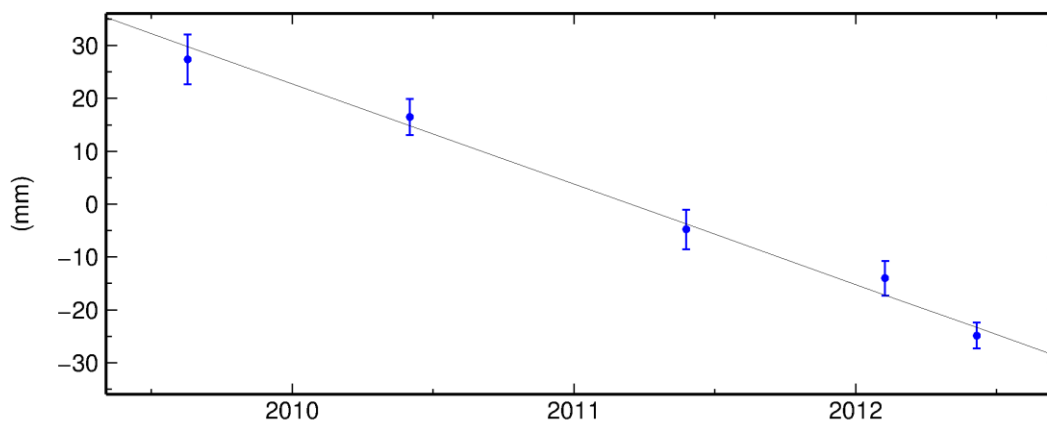
KPLC East Offset   2357631.702 m
rate(mm/yr)= −17.73 ± 1.34 nrms= 0.64 wrms= 1.9 mm # 5
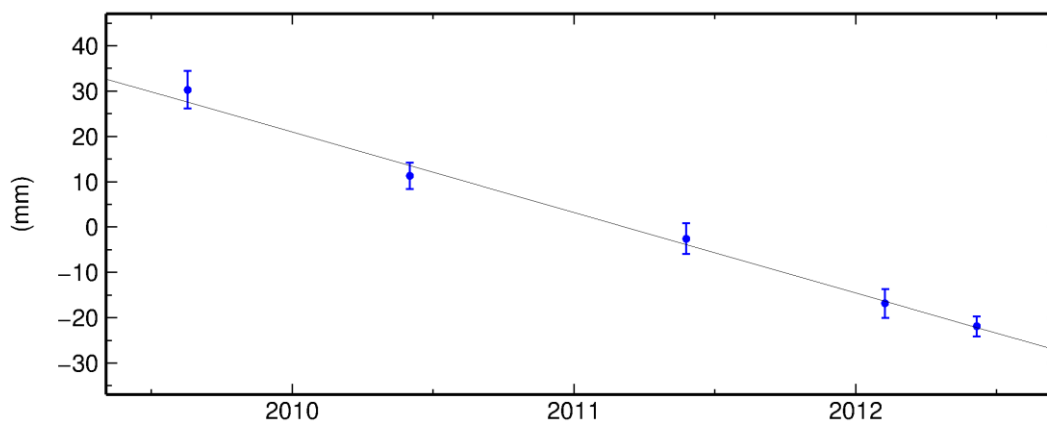
KPLC Up Offset   48.019 m
rate(mm/yr)= 32.65 ± 6.06 nrms= 3.66 wrms= 48.2 mm # 5
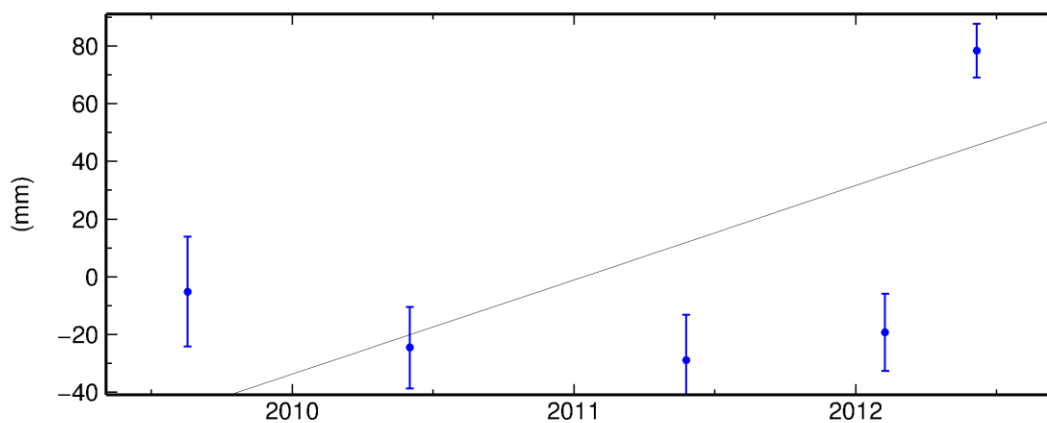
PTKV North Offset   4253402.681 m
rate(mm/yr)= −15.29 ± 1.62 nrms= 0.55 wrms= 2.0 mm # 5
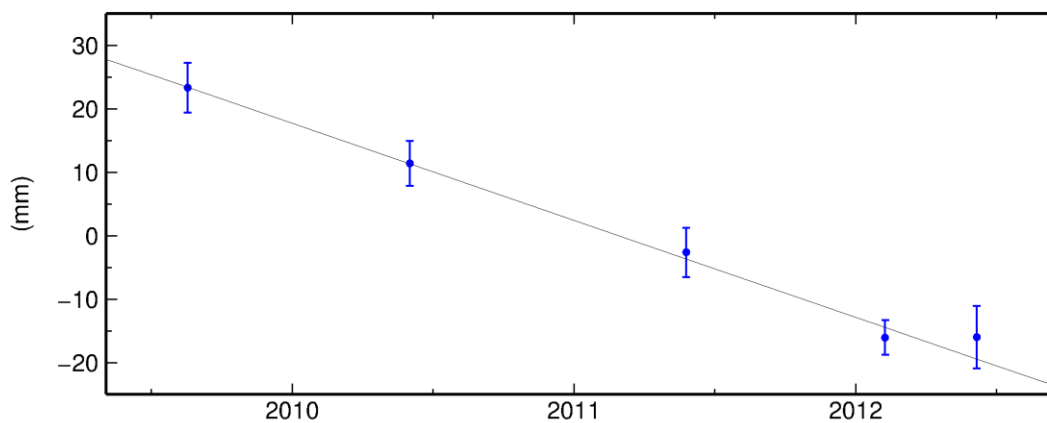
PTKV East Offset   2362746.573 m
rate(mm/yr)= −20.35 ± 1.49 nrms= 0.35 wrms= 1.2 mm # 5
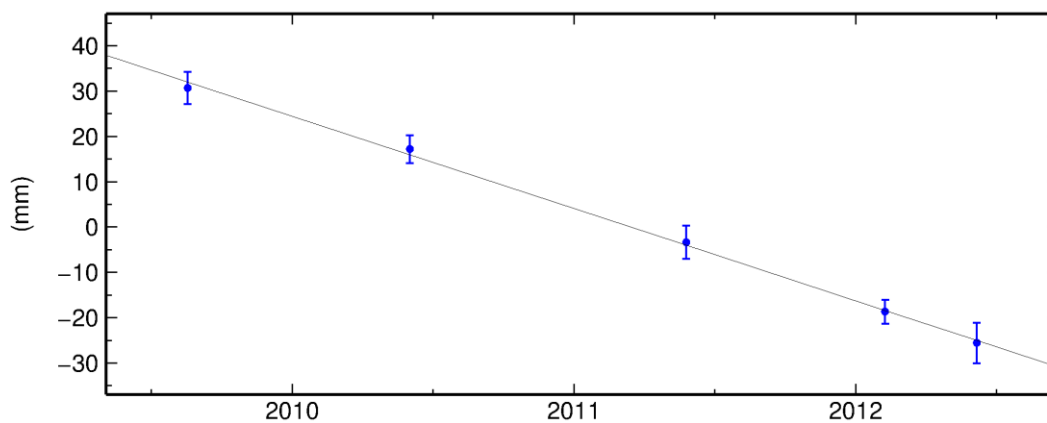
PTKV Up Offset   286.403 m
rate(mm/yr)= −0.38 ± 6.59 nrms= 0.28 wrms= 4.2 mm # 5

GMD 2012 Jul 09 17:22:46   p: 18
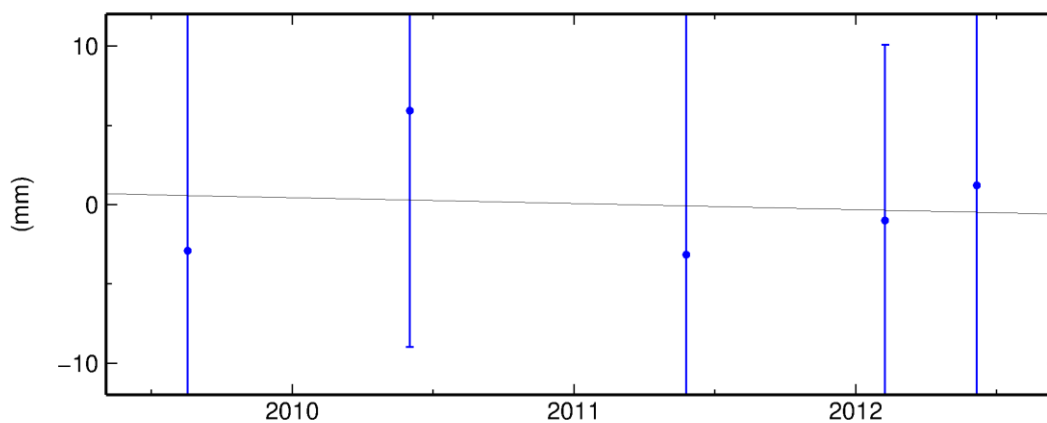
SFRH North Offset   4254121.204 m
rate(mm/yr)= −15.62 ± 1.46 nrms= 1.37 wrms= 4.4 mm # 5
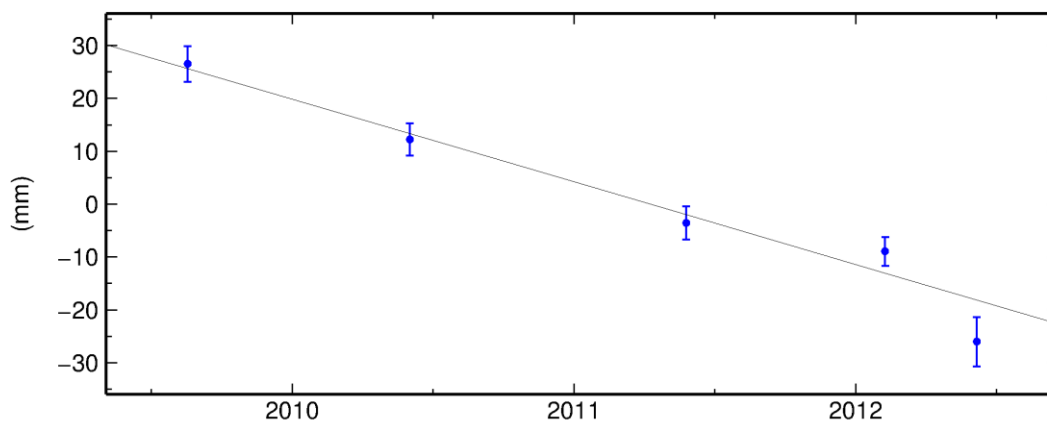
SFRH East Offset   2343740.918 m
rate(mm/yr)= −17.08 ± 1.37 nrms= 0.52 wrms= 1.6 mm # 5
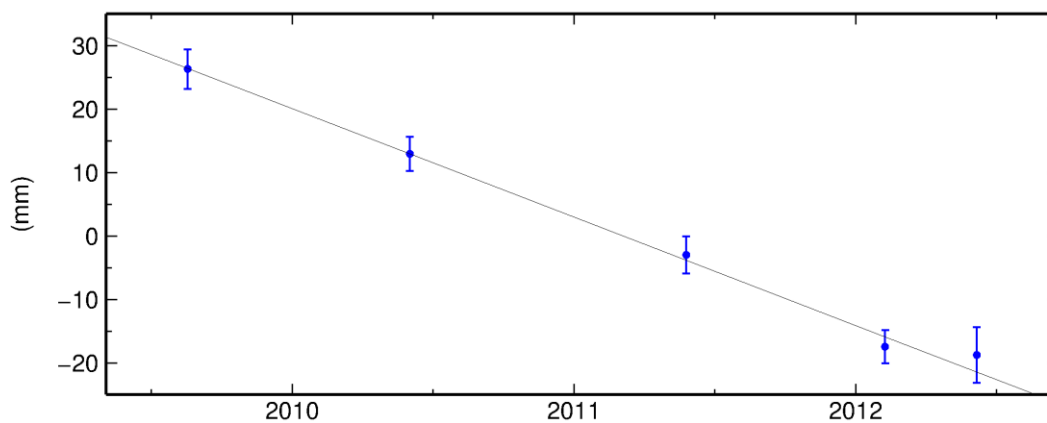
SFRH Up Offset   145.934 m
rate(mm/yr)= −2.66 ± 6.01 nrms= 0.81 wrms= 10.9 mm # 5

GMT 2012 Jul 09 17:22:46   p: 19
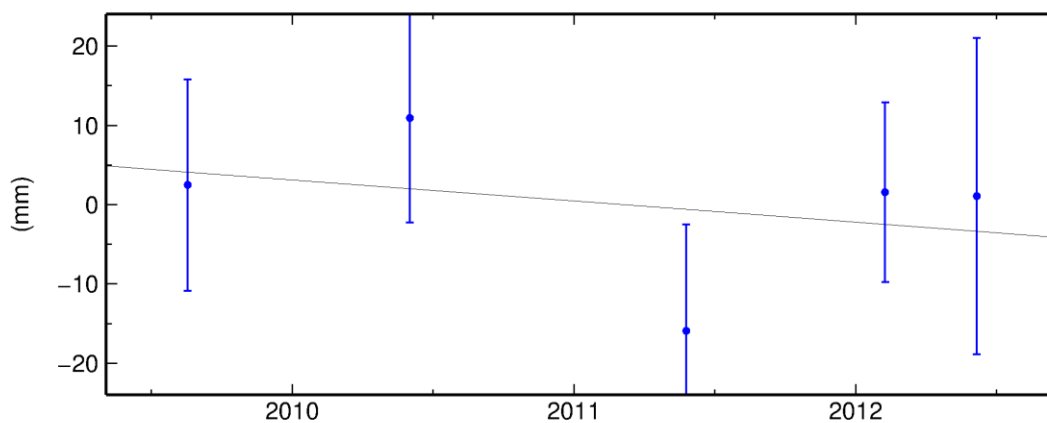
TRAZ North Offset   4259853.044 m
rate(mm/yr)= −14.35 ± 1.52 nrms= 0.97 wrms= 3.3 mm # 5
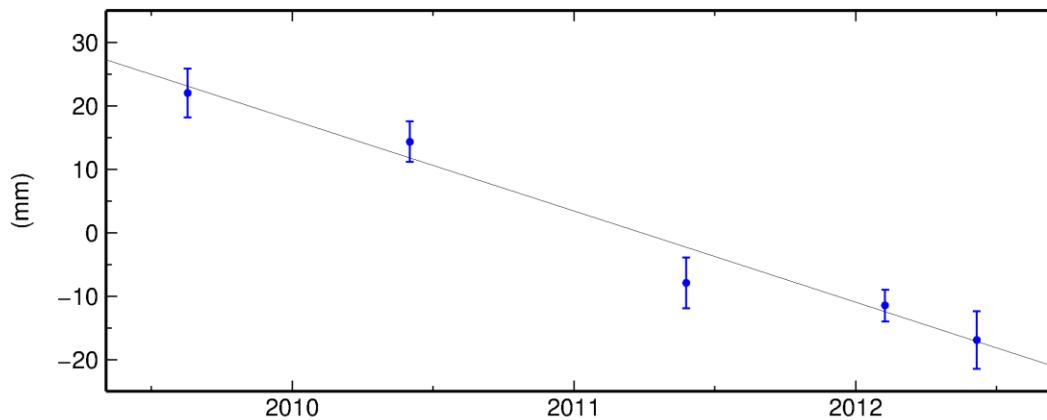
TRAZ East Offset   2359410.717 m
rate(mm/yr)= −19.66 ± 1.36 nrms= 0.42 wrms= 1.3 mm # 5
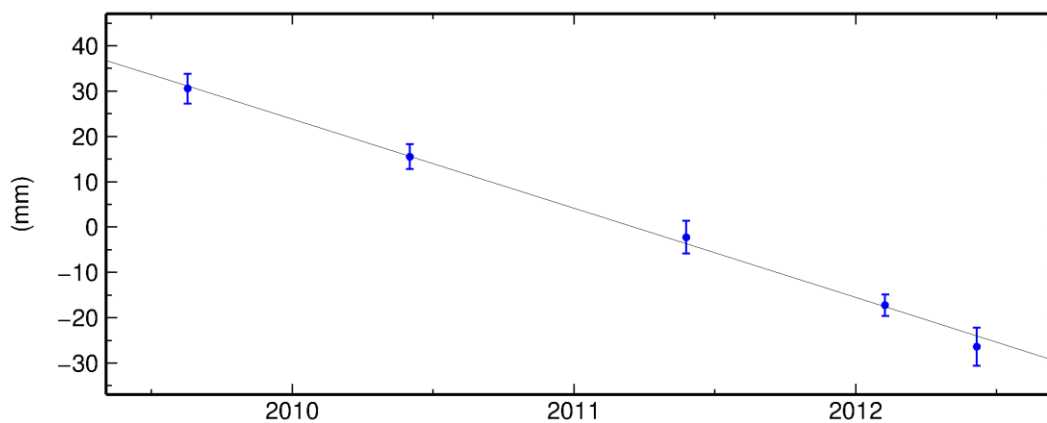
TRAZ Up Offset   824.550 m
rate(mm/yr)= −4.56 ± 5.94 nrms= 0.46 wrms= 6.3 mm # 5

GMT 2012 Jul 09 17:22:48   p: 21
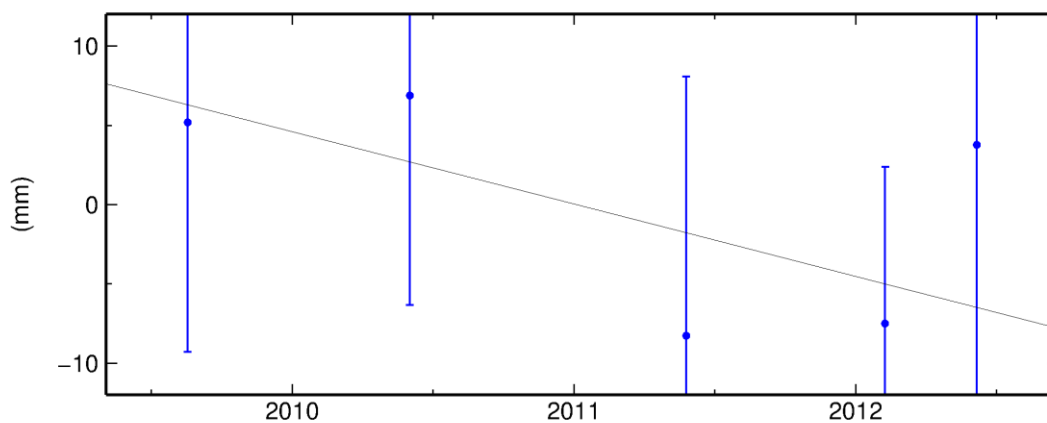
TURG North Offset   4259627.147 m
rate(mm/yr)= −18.41 ± 1.48 nrms= 0.60 wrms= 1.7 mm # 5
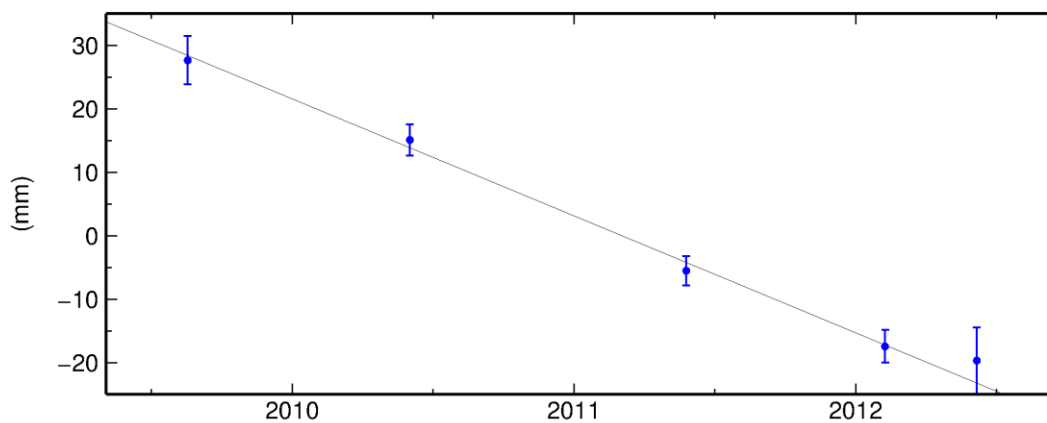
TURG East Offset   2340783.041 m
rate(mm/yr)= −18.31 ± 1.35 nrms= 0.73 wrms= 1.9 mm # 5
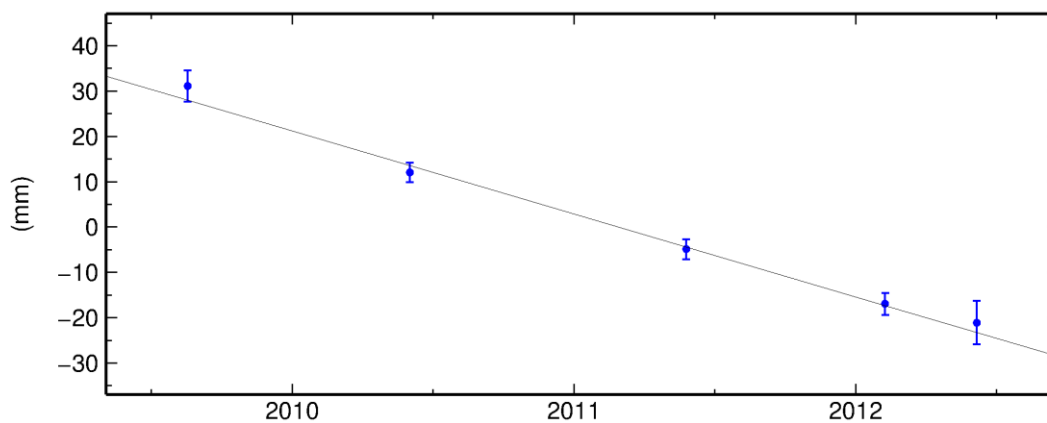
TURG Up Offset   137.975 m
rate(mm/yr)= −2.94 ± 5.89 nrms= 0.88 wrms= 10.1 mm # 5

GMT 2012 Jul 09 17:22:49   p: 23
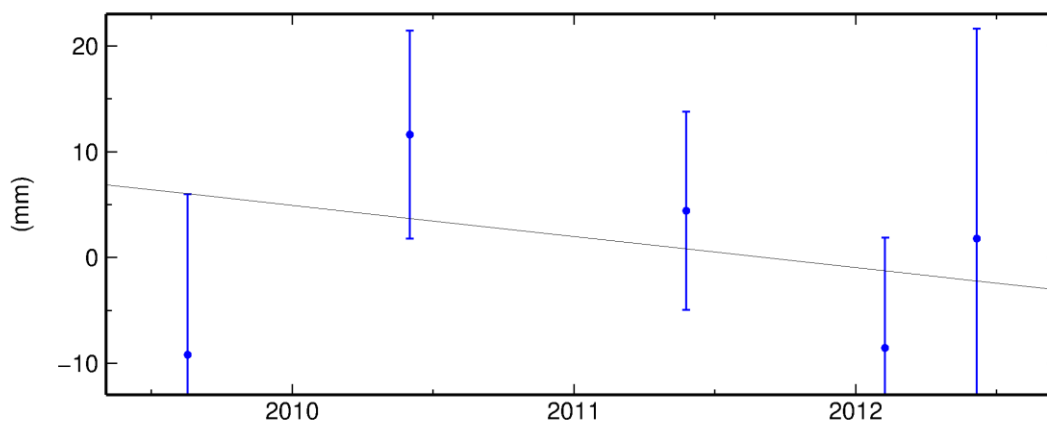
URKM North Offset   4240433.965 m
rate(mm/yr)= −17.59 ± 1.36 nrms= 0.96 wrms= 2.9 mm # 5
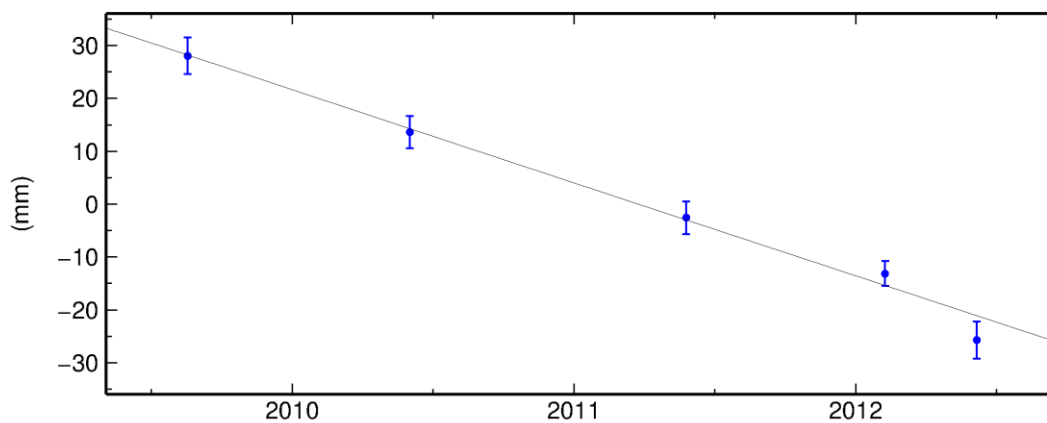
URKM East Offset   2360965.927 m
rate(mm/yr)= −18.88 ± 1.23 nrms= 0.79 wrms= 2.2 mm # 5
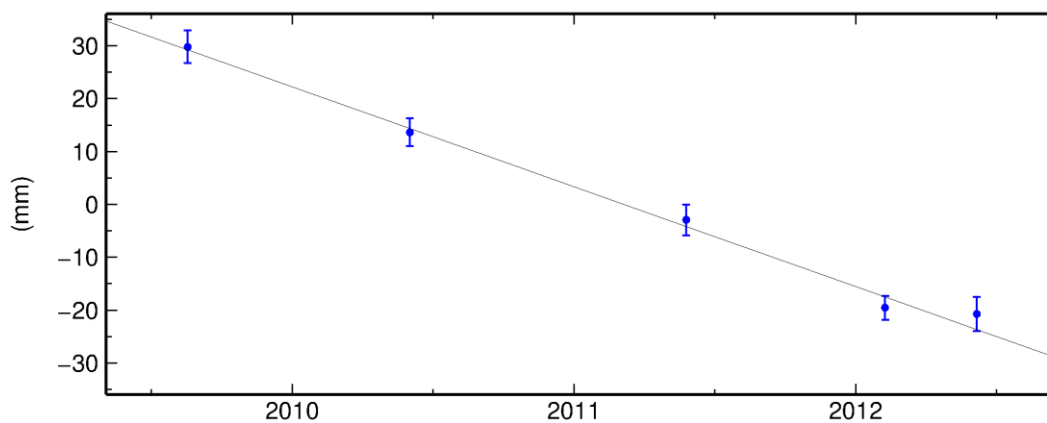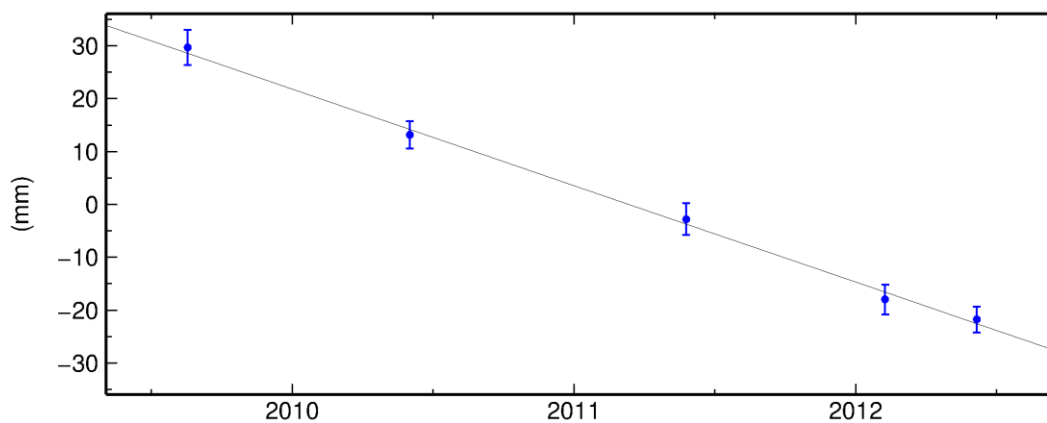

URKM Up Offset   76.499 m
rate(mm/yr)= −5.60 ± 5.32 nrms= 0.54 wrms= 6.5 mm # 5

GMD 2012 Aug 23 11:48:53   p: 24
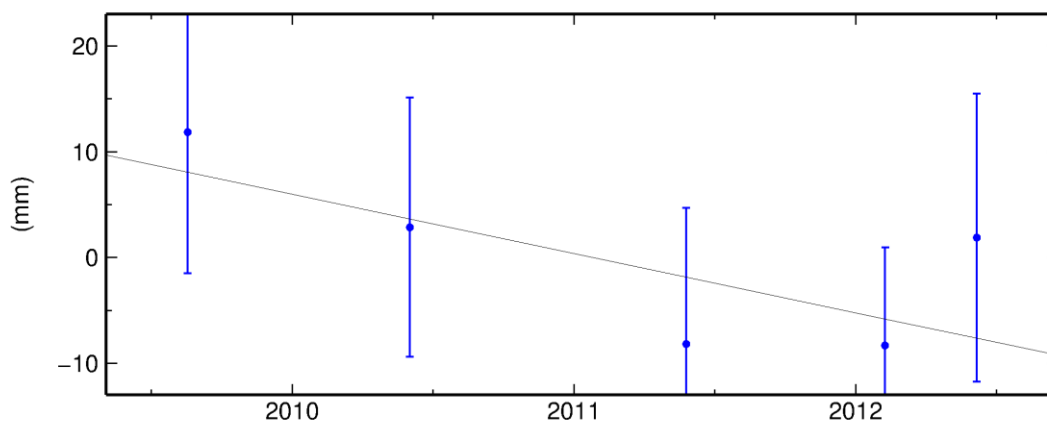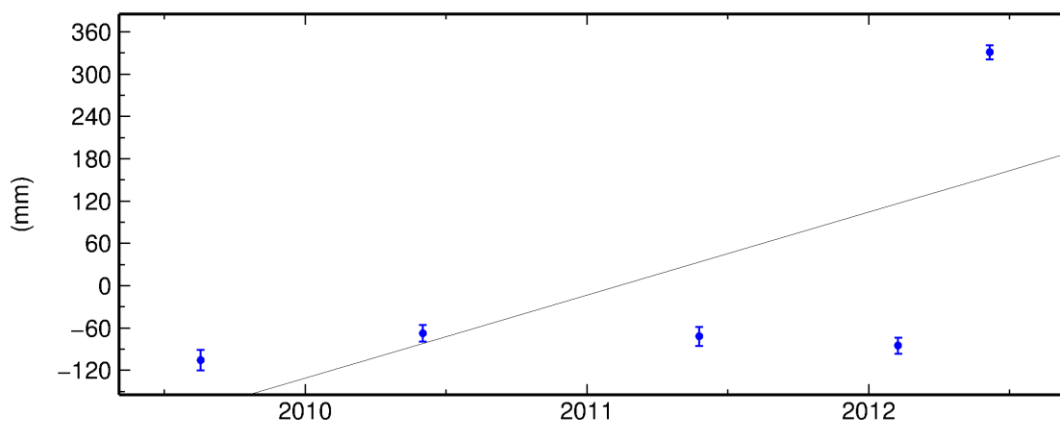
YACI North Offset   4255657.996 m
rate(mm/yr)= −16.81 ± 1.38 nrms= 0.78 wrms=   2.4 mm # 5
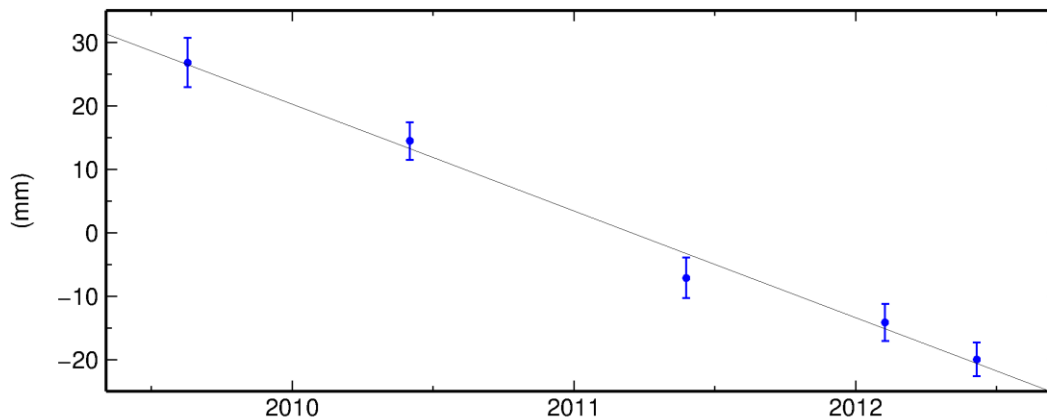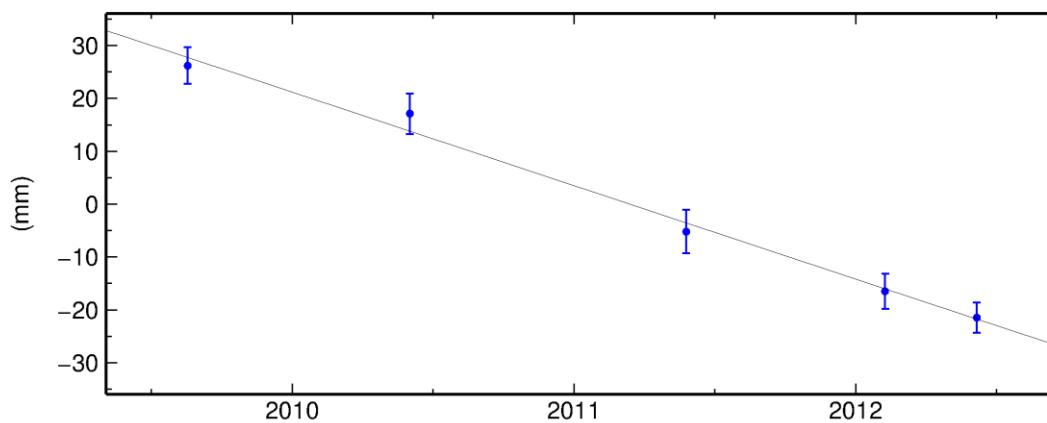

YACI East Offset   2331083.323 m
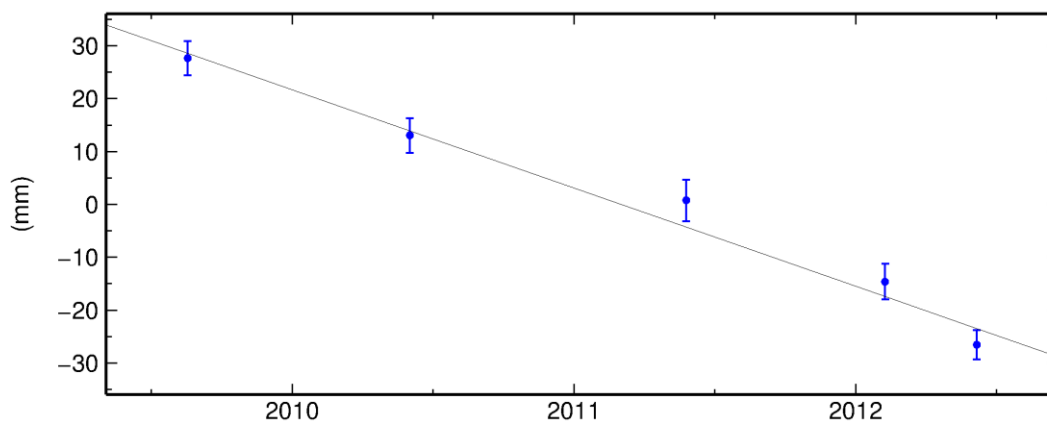rate(mm/yr)= −18.25 ± 1.23 nrms= 0.48 wrms=   1.3 mm # 5

YACI Up Offset   250.472 m
rate(mm/yr)= 117.74 ± 5.27 nrms= 15.48 wrms= 184.8 mm # 5

GMT 2012 Jul 09 17:22:50   p: 25

YKOY North Offset   4254156.159 m
rate(mm/yr)= −17.64 ± 1.41 nrms= 0.61 wrms= 2.1 mm # 5

YKOY East Offset   2364624.037 m
rate(mm/yr)= −18.57 ± 1.33 nrms= 1.12 wrms= 3.6 mm # 5

YKOY Up Offset   259.516 m
rate(mm/yr)= 15.14 ± 5.93 nrms= 1.26 wrms= 18.4 mm # 5

GMT 2012 Jul 09 17:22:51   p: 26